Proudman
Oceanographic
Laboratory

The heat balance of the North Sea

A Lane

Report No 8 1989

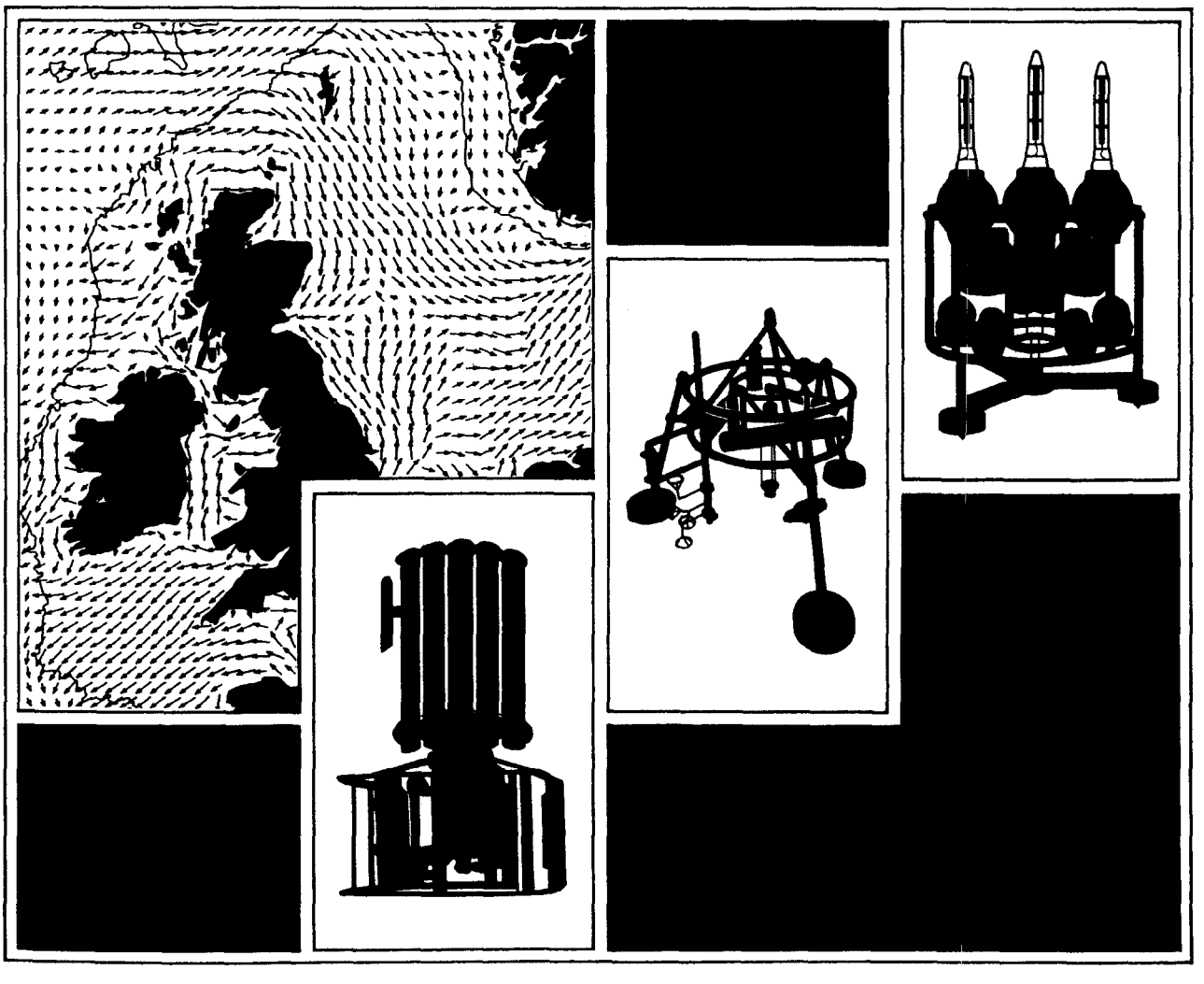

Natural Environment Research Council

PROUDMAN OCEANOGRAPHIC LABORATORY

Bidston Observatory,
Birkenhead, Merseyside, L43 7RA, U.K.

Telephone: 051 653 8633
Telex 628591 OCEANB G
Telefax 051 653 6269

Director: Dr. B.S. McCartney

Natural Environment Research Council

PROUDMAN OCEANOGRAPHIC LABORATORY

REPORT No. 8

The heat balance of the North Sea

A. Lane

1989

DOCUMENT DATA SHEET

AUTHOR	PUBLICATION DATE
LANE, A.	1989

TITLE

The heat balance of the North Sea

REFERENCE

Proudman Oceanographic Laboratory, Report No. 8, 46 pp.

ABSTRACT

Equations from Goldsmith and Bunker (WHOI 1979) which describe the heat exchange processes between the sea surface and the atmosphere are presented. The component parts of these equations involve: R_s, the solar radiation at the sea surface; L_e, the latent heat flux; IR, the effective infra-red back radiation; and S, the sensible heat flux. The dependence of these equations on certain parameters is examined, with the intention of using them in simulating the heat balance of the North Sea.

Using parameter values appropriate to the North Sea, that is, an air temperature of 11.0°C, sea surface temperature of 11.6°C, dew-point temperature of 8.3°C, wind speed 7.8 m s^{-1}, 101392 Pa atmospheric pressure and 5.6 Okt cloud cover; the sensitivity of the net annual heat flux is analysed for small perturbations from these mean values. This analysis shows that overall, the difference between mean air and sea surface temperature is of vital importance. It is shown that a change in mean air temperature of 1°C is likely to be accompanied by a 0.5°C change in mean sea surface temperature. An interesting result was found concerning the variation in the solar radiation flux with both latitude and season. Thus, at its maximum in July, this component shows little north-south variation within the North Sea dimensions; while at its minimum in January, the southern limit receives appreciably more energy. Thus the observed north-south gradient in mean temperature in the North Sea may be attributed in part to this variation in direct heating - as well as to the influence of south to north advection of adjacent oceanic waters.

ISSUING ORGANISATION	TELEPHONE
Proudman Oceanographic Laboratory Bidston Observatory Birkenhead, Merseyside L43 7RA UK Director: Dr B S McCartney	051 653 8633
	TELEX 628591 OCEAN B
	TELEFAX 051 653 6269

KEYWORDS	CONTRACT
HEAT BUDGET NORTH SEA PROJECT NWEURNOR NORTH SEA	PROJECT MNS3 12
	PRICE £14

CONTENTS

1 INTRODUCTION

At present, there is much interest in climatic change, especially changes in atmospheric gases and their related effect on wind speed, humidity and air and sea surface temperatures. Whilst many studies of the global ocean-atmosphere feedback are currently being undertaken, the research described here examines effects over smaller shallow seas - specifically the North Sea. In subsequent phases, this study will use data from the North Sea Project in conjunction with detailed numerical models of both circulation and stratification (i.e., vertical mixing) of the sea.

Although there are many empirical formulations of the heat exchange equations, the equations listed in the 1979 WHOI technical report of Goldsmith and Bunker form the basis of this examination of the heat balance at the sea surface. Diagrammatic representations were produced showing the dependency of the total heat flux on the primary variables, i.e., air temperature and sea surface temperature. The sensitivity of these relationships to subsidiary variables was then examined, namely, time of year, latitude, atmospheric pressure, cloud cover and wind speed (figure 1).

Before investigating long term changes using these models, the sea-atmosphere exchange processes must first be understood - in particular, the interdependency of the component processes. For example, if there is an increase in air and sea temperatures, will possible changes in cloud cover or humidity invalidate the simulation? There is also interest in the sensitivities of these processes to certain parameters, e.g., the heat exchange coefficient. The basic features and sensitivities of the component exchange processes are the subject of this report.

2 HEAT EXCHANGE AT THE SEA SURFACE

The four major components of the heat balance, in order of importance, are as follows:

i) R_s, Solar radiation at the sea surface; this is the main mechanism by which the sea gains heat.

ii) L_e, Latent heat flux; this is the heat loss by evaporation, and in certain conditions, heat gain by condensation.

iii) IR, Effective infra-red back radiation; the sea behaves almost as if it is a black body. The radiation it emits is absorbed by atmospheric water vapour from where it is re-emitted. The effective back radiation is the difference between the initial back radiation of the sea and the re-radiation of the atmosphere in the direction of the sea surface.

iv) S, Sensible heat flux; this is the heat exchange of the sea and air by conduction across the interface.

The heat balance at the sea surface, H_x, is given by

$$H_x = R_s - L_e - IR - S \qquad (1)$$

i.e. the solar radiation term minus the sum of the latent heat, effective back radiation and sensible heat terms.

Each of the four heat exchange mechanisms are considered below for a range of values of (i) air temperature, (ii) sea surface temperature, (iii) atmospheric pressure and (iv) wind speed. It was assumed that the air directly above the sea surface would be saturated: the dew-point temperature was set to be 0.1°C below the air temperature, corresponding to a relative humidity of about 99%. This is so as to ensure consistency with Goldsmith & Bunker's conditions for the validation of data.

2.1 The solar radiation flux

Radiation from the Sun corresponds to a black body radiation of approximately 5800 K, which has a maximum of emission at a wavelength of about 500 nm. The heat flux normal to its direction of incidence (at the mean earth-sun distance), at the top of the atmosphere, is given by the solar constant as 1.35 kW m^{-2}. The radiation spectrum is modified as it passes through the atmosphere; by scattering, reflection by cloud cover, absorption and re-radiation by water vapour and carbon dioxide in the infra-red, oxygen O_2 and O_3 in the visible and ultra-violet respectively (DEFANT, 1961).

The apparent thickness of the atmosphere depends on the aspect of the sun. This varies with latitude and the time of year. The incident solar radiation flux, Q is tabulated in table 1. The solar radiation which is reflected by the sea surface is proportional to its albedo, a_s (table 2), which is also dependent on latitude and season.

The solar radiation flux in W m^{-2}, R_s in terms of the cloud cover, $\overline{N}_t$ and albedo, a_s is given as

$$R_s = Q\,(1 - {}^1/_8\overline{N}_t\, c_s - 0.38 \cdot {}^1/_{64}\overline{N}_t^2)(1 - a_s) \qquad (2)$$

where c_s is the solar radiation cloud cover coefficient (table 3).

The effect of cloud cover is to reduce the magnitude of the solar radiation flux reaching the sea surface. Table 4 gives the proportion of radiation reflected or absorbed, by cloud cover from 1.0 to 8.0 Okt.

The annual cycle of the solar radiation flux (figure 2) shows the presence of a heat flux gradient which varies with season. In the North Sea between 51° and 57°N, for a mean cloud cover of 5.6 Okt, there is a gradient of approximately 2.1 W m^{-2} deg lat^{-1} in January; in July this is approximately 1.4 W m^{-2} deg lat^{-1} (table 5).

2.2 The latent heat flux

This is the second most important of the heat exchange mechanisms accounting for around 54% of the total heat loss. A net evaporation occurs whenever the air above the sea surface is not saturated. When the air is heated by the sea, the relative humidity decreases, allowing further evaporation. The effect of the wind is to increase the evaporation rate by moving the saturated air away from the sea surface.

Less commonly, the condensation rate exceeds that of evaporation when the air over the sea surface is supersaturated and the sea gains heat, for sea surface temperatures less than the air temperature.

The latent heat flux in W m^{-2}, L_e is given by

$$L_e = (250097.8 - 2365.09\ t_a)\ \rho\ W\ (q_s - q_a)\ C_e(t_{as},W) \qquad (3)$$

where W is wind speed /m s^{-1}
t_{as} is the air-sea temperature difference /°C
$C_e(t_{as},W)$ is the exchange coefficient

Figure 3 shows the plots obtained by using equation (3) for the unsaturated and saturated cases. The relationship between the latent heat flux and the air and sea temperatures is modulated by the exchange coefficient C_e, which is a function of the air-sea temperature difference t_{as} and the wind speed W. The values of C_e are extracted from table 6, for ranges of t_{as} and W. The plots are sensitive to the value of C_e, and hence are particularly uneven. This effect can be seen clearly in figures 3a and 3b. The irregularities were reduced when the values of the exchange coefficient were linearly interpolated for t_{as}. The dependence of the latent heat flux on wind speed is shown in figure 4.

Figure 5 indicates that there is little dependence of the latent heat flux on atmospheric pressure. A worst case analysis of the parameter ρ gives $\rho T_a \simeq 334.9 \pm 10\%$ K kg m^{-3}. This is the extreme range of values allowed under the conditions for the validation of data.

The contour plots showing the above properties also show that for high air and sea surface temperatures, the latent heat flux is large and sensitive to changes in the air and sea surface temperatures. In the region where temperatures are near those usually encountered in the North Sea (0° to 20°C), however, the heat flux is not as sensitive to temperature changes.

2.3 The effective infra-red back radiation

The black body radiation of the sea surface at a temperature of 10°C has a maximum at a wavelength of 10 μm. Approximately 50% of this radiation spectrum coincides with the infra-red spectrum of atmospheric water vapour and carbon dioxide (figure 6), and is absorbed and re-emitted. The re-radiation takes place in random directions and some of this is

re-absorbed by the sea. In addition to this, water vapour and CO_2 in the air also re-radiates the solar radiation absorbed in the infra-red region of the spectrum (see section 2.1).

The amount of heat loss by effective infra-red back radiation is therefore dependent on the relative humidity which determines the amount of water vapour in the air and hence the proportion of heat absorbed and re-emitted. It is thus dependent on the amount of cloud cover, which reflects the radiation.

The infra-red back radiation flux of the sea in W m^{-2}, at a temperature T_s in an environment at temperature T_a, is

$$IR_s = \epsilon \sigma T_s^4 - \alpha \sigma T_a^4 \qquad (4)$$

where $\sigma = 1.3134 \times 10^{-9}$ W m^{-2} K^{-4} (Budyko's modified value for Stefan-Boltzmann constant)
$\epsilon = 0.96$, spectral emissivity and
$\alpha = 0.96$, absorptance

For $(T_s - T_a) \simeq 0$, this is approximately $4 \epsilon \sigma T_a^3 (T_s - T_a)$. Here the emissivity ϵ is assumed to be equal to the absorptance α, as the sea is not a perfect black body. ϵ and σ are given by Goldsmith & Bunker to be 0.96 and 1.3134×10^{-9} W m^{-2} K^{-4} respectively, where σ is Budyko's modified value.

An empirical equation for the effective back radiation, which takes into account the complex atmospheric absorption and radiation is

$$IR = 0.96 \sigma T_a^4 (11.7 - 0.0023 P_d)(1 - {}^1/_8 \overline{N}_t c_c) + 3.84 \sigma T_a^3 (T_s - T_a) \qquad (5)$$

where c_c is the cloud cover coefficient (table 7)
$\overline{N}_t$ is the average cloud cover in eighths

The black body radiation of the sea itself is small, being some three orders of magnitude less than the atmospheric radiation term, at air temperature $t_{as} = 11.0°C$ and air-sea temperature difference $t_{as} = -0.6°C$. The plots of the effective back radiation produced from

equation (5) show that the back radiation is more sensitive to changes in air temperature than sea surface temperature, and its sensitivity to sea surface temperature increases with increasing cloud cover (figure 7). In the situation where the relative humidity is high, there is a net heat gain for high air temperatures (figure 8). The back radiation is relatively insensitive to temperature changes in the temperature range 0° to 20°C as in section 2.2 above.

2.4 The sensible heat flux

This concerns the heat transfer by conduction only, and represents about 8% of the total heat loss. The sensible heat flux is proportional to the air-sea temperature difference t_{as}, and wind speed W (figure 9). For positive values of t_{as}, heat is gained by the sea, and vice versa. Note that the air gains heat at a greater rate than the sea, a consequence of their thermal conductivities, i.e., 0.026 and 0.60 W m^{-1} K^{-1} respectively.

The sensible heat flux in W m^{-2}, is given by

$$S = -t_{as}\ \rho\ W\ C_p\ C_e(t_{as},W) \qquad (6)$$

where C_p = 1004.64 J kg^{-1} K^{-1}

Figure 10 shows that the sensible heat flux is insensitive to changes in the dew-point temperature, whereas figure 11 shows that its dependence upon pressure is negligible, for the same reason as that described for the latent heat flux above.

3 OBSERVATIONS AT NOORD HINDER

In this report, data appropriate to the North Sea were extracted from the Bunker Climate Atlas (ISEMER & HASSE 1985). In order to assess their accuracy, a comparison is made between these data and a year-long set of observations from the Dutch light vessel Noord Hinder moored at 51° 39'N, 2° 33'E in the southern North Sea (figure 12). The observed annual mean values of air and sea surface temperatures, atmospheric pressure and dew-point temperature are higher by 1.7°C, 1.8°C, 7 Pa, and 1.8°C respectively (figure 13).The data from

the Bunker Atlas refer strictly to the region 55 - 57°N, 3 - 5°E and hence these discrepancies may be partly due to the north-south gradient (see section 2.1). However, the overall agreement is sufficient to proceed to a sensitivity analysis described in section 4 in which small perturbations about the above annual means are considered. Observed data of air and sea surface temperatures, atmospheric pressure and humidity for the period 1st January to 31st December 1977 were analysed. The means and standard deviations of these parameters are shown in table 8. The wet-bulb temperature is given in the data, instead of the dew-point temperature. Its relationship to the relative humidity is (KAYE & LABY 1989)

$$RH/\% = 100 \times (P_w - A\, P_{atm}\, (t_a - t_w))/P_a \qquad (7)$$

where P_w is the saturated vapour pressure at temperature t_w
P_a is the saturated vapour pressure at temperature t_a
P_{atm} is total atmospheric pressure
$A = 0.000666°C^{-1}$ for a force-ventilated psychrometer

The average relative humidity is 83.8% with a standard deviation of 8.5 (± 10%). The correlation between the air temperature, t_a and the wet-bulb temperature, t_w is 0.9813, so the two variables are closely related. The wet-bulb temperature was set to be 1.41°C below the air temperature. (1.41°C is the mean wet-bulb depression.) The average relative humidity in this case was found to be 83.5% with a standard deviation of 2.7 (± 3%). Thus the assumption in section 2, that the relative humidity is essentially constant seems sensible, but it is not as high as 99%. The linear regression of the wet-bulb temperature on the air temperature gives a linear relationship between the two variables to be $t_w = 0.956\, t_a - 0.927$.

4 SENSITIVITY ANALYSIS

In order to assimilate the detailed results given above, and examine the effect of changes in the various components of climate, on the air-sea heat transfer, this section investigates the effects of *independently* varying the following (in relation to the conditions at Noord Hinder 51°N):

i) t_a, the average air temperature by -2°, -1°, 1°, 2°C.

ii) t_s, the average sea surface temperature by -2°, -1°, 1°, 2°C.

iii) t_d, the average dew-point temperature by -1.4°, 1.4°, 2.8°C.

iv) W, the average wind speed by -3, -1.5, 1.5, 3 m s^{-1}.

v) P_{atm}, the average atmospheric pressure by -1000, 1000 Pa.

vi) $\overline{N}_t$, the average cloud cover by -1, 1, 2 Okt.

The effect on each component of heat flux of the above conditions is given in tables 4 and 9. These are obtained by treating each of these changes as though they were independent of each other. Table 10 shows values calculated for varying the air and sea surface temperatures together. In describing these tabulated results, the sensitivity of each component of the heat flux to specific parameters is highlighted.

The solar radiation flux

The solar radiation flux is sensitive to the amount of cloud cover. The average cloud cover at present in the southern North Sea (51°N) is 5.6 Okt with a corresponding average annual solar radiation flux of 106 W m^{-2}. An increase in cloud cover by one Okta reduces this radiation flux by about 24 W m^{-2} (to 82 W m^{-2}). A decrease of one Okta increases the radiation flux by 22 W m^{-2} (to 128 W m^{-2}). The solar radiation flux is independent of the remaining parameters.

The latent heat flux

This is more sensitive to sea surface temperature than to air temperature. A one degree increase in air temperature above the present mean of 11.0°C decreases the heat loss from its present value of 55.4 W m^{-2} by about 4 W m^{-2}. Whereas a one degree increase in sea surface temperature above the present mean of 11.6°C increases the heat loss from 55.4 W m^{-2} by about 25 W m^{-2}.

The amount of heat exchange by this mechanism depends strongly on the evaporation and condensation rates which in turn depend on the relative humidity. The present value (55.4 W m^{-2}) of latent heat flux at 83% relative humidity becomes 82.7 W m^{-2} at a humidity of 75% and 9.8 W m^{-2} at 99%. An increase of 1.5 m s^{-1} for the wind speed is accompanied by an increase of heat flux of approximately 15 W m^{-2}, a decrease of wind speed by 1.5 m s^{-1}

decreases the heat flux by approximately 11 W m^{-2}. Dependence on atmospheric pressure and cloud cover is negligible.

The effective infra-red back radiation

Relative to the latent heat flux, the effective IR back radiation is insensitive to changes in air, sea surface and dew-point temperatures, with less than 1 W m^{-2} variation for the parameter variations considered. It is only sensitive to changes in cloud cover varying from its present mean of 37.5 W m^{-2} by about 7 W m^{-2} for a one Okta change.

The sensible heat flux

The Sensible heat flux is sensitive only to air and sea surface temperatures, and wind speed. Its relationship to the air temperature is approximately linear for small changes in air and sea surface temperatures. Thus an increase in air temperature of one degree decreases the heat flux by 14.3 W m^{-2} to -5.5 W m^{-2} whilst a decrease of one degree increases the value by 16.3 W m^{-2} to 25.1 W m^{-2}.

The total heat exchange

The total heat exchange is shown to be insensitive to independent changes in either mean dew-point temperature or atmospheric pressure (figures 14 and 15 respectively). The changes indicated in table 9 for the latter refer to exceptionally large variations in this parameter. Similarly, both mean cloud cover and mean wind speed can vary substantially without radical changes in the net heat flux (figures 16 and 17). In contrast, a 1°C change in either air or sea surface temperature significantly modifies the net heat exchanges, both effects being linear for a few degrees change. The influence of a change in air temperature is approximately twice that of a change in sea surface temperature.

With reference to table 10, the apparent sensitivity to sea surface and air temperature changes noted above, is qualified by examining simultaneous changes in these parameters. The

table shows that if a change in air temperature of 2°C is accompanied by a corresponding change in sea surface temperature of 1°C, the net heat flux remains little changed.

Neglecting advection in the sea, the net heat flux must be close to zero and hence any long term study of trends in sea surface temperatures of the North Sea must involve an examination of the interdependence of air and sea surface temperatures.

These effects on net heat exchange mask the differing separate effects of the latent heat flux and the sensible heat flux - the infra-red component remains little changed. Thus while the sensible heat flux remains unchanged for equal changes in air and sea surface temperatures, the latent heat flux is particularly sensitive to sea surface temperatures and relatively insensitive to air temperature. The additional sensitivity to wind speeds is noted in the earlier separate discussions of these components. Clearly, any net imbalance between air and sea surface temperatures can modify local wind conditions.

5 CONCLUSION

This report shows that the air-sea heat exchange processes are complex; they are dependent on empirical coefficients and the forcing parameters are interdependent.

The above algorithms are to be incorporated within a numerical model in order to simulate the observed annual cycle of temperature distribution, as part of the North Sea Project. This model will include advection and stratification. Assuming the success of this simulation, attempts will be made to reproduce the observed inter-annual variability. As a result of this, some of the interdependence of the forcing parameters may be revealed.

The aim is to be able to predict the future sea temperature distribution as a function of various climatic situations and to examine the importance of ocean/shelf sea thermal exchanges in that respect.

5.1 References

DEFANT, A. 1961

Physical Oceanography. Volume 1.
Oxford: Pergamon Press. 729pp.

GOLDSMITH, R.A. & BUNKER, A.F. 1979

Woods Hole Oceanographic Institution collection of climatology and air-sea interaction (CASI) data.
Woods Hole Oceanographic Institution, Technical Report WHOI-79-70, 75pp.

ISEMER, H-J. & HASSE, L. 1985

The Bunker climate atlas of the North Atlantic Ocean.
Volume 1. Observations.
Berline: Springer-Verlag, 218pp.

KAYE, G.W.C. & LABY, T.H. 1986

Tables of physical and chemical constants and some mathematical functions. (15th edition).
London: Longman. 477pp.

OTTO, L. 1981

Meteorological and oceanographic observations on board Netherlands lightvessels and the light platform 'Goeree' in the North Sea.
Koninklijk Nederlands Meteorologisch Institut, Jaargang 29-1977, 107pp.

PRANDLE, D. & JOHNSON, R. 1988

Some explanations for the stability of annual temperature variations in the North Sea and some indications of their sensitivity to the Greenhouse Effect. (Unpublished manuscript)

LIST OF SYMBOLS

Symbol			*units*
t_a, T_a	air temperature	$T_a = t_a/°C + 273.16$	°C, K
t_s, T_s	sea surface temperature	$T_s = t_s/°C + 273.16$	°C, K
t_d, T_d	dew-point temperature	$T_d = t_d/°C + 273.16$	°C, K
t_w, T_w	wet-bulb temperature	$T_w = t_w/°C + 273.16$	°C, K
t_{as}	air-sea temperature difference	$t_{as} = t_a - t_s$	°C
P_{atm}	atmospheric pressure		Pa
W	wind speed		$m\ s^{-1}$
$\overline{N}_t$	average cloud cover in eighths		Oktas
C_p	specific heat capacity of dry air		$J\ K^{-1}\ kg^{-1}$
σ	Stefan-Boltzmann constant		$W\ m^{-2}\ K^{-4}$
ϵ, α	spectral emissivity, spectral absorptance		

The following are defined in the Appendix

P_d	saturated vapour pressure of air at the sea surface	Pa
P_s	vapour pressure over sea	Pa
q_a	mixing ratio of air	
q_s	mixing ratio of air over sea	
ρ	density of air over sea	$kg\ m^{-3}$

The following are given in Tables 1, 2, 3, 6 and 7

Q	solar radiation flux at bottom of atmosphere	$W\ m^{-2}$
a_s	sea surface albedo coefficient	
c_s	solar radiation cloud cover coefficient	
C_e	exchange coefficient	
c_c	back radiation cloud cover coefficient	

APPENDIX

Saturated vapour pressure of air P_d at the sea surface

$$\log P_d = c_1 + c_2/T_d + c_3/T_d^2$$

$c_1 = 10.42926609$

$c_2 = -1.82717842 \times 10^3$

$c_3 = -0.071208271 \times 10^6$

Vapour pressure over sea P_s [1]

$$\log P_s = c_1 + c_2/T_s + c_3/T_s^2 + c_4$$

$c_4 = -0.008774$

Ratios q_a of air, q_s of air over sea [2]

$$q_a = 0.662\ P_d / (P_{atm} - P_d)$$

$$q_s = 0.662\ P_s / (P_{atm} - P_s)$$

Density of air ρ over sea [3]

$$\rho = P_{atm} / (287.04\ T_a\ (1 + 0.61\ q_a))$$

---

[1] For t_d, $t_s \leq 40^oC$, P_d and $P_s \leq 7390$ and 7240 Pa respectively. Compared with atmospheric pressure, (minimum considered 89000 Pa) - this is a deviation of approximately 8.3%.

[2] t_d/P_{atm} for constant q_a, is approximately 2×10^{-4} °C Pa^{-1}. From a plot of q_a, in terms of pressure P_{atm} and t_d, q_a is essentially constant for a small change of P_{atm}.

[3] For a fixed amount of air, its volume is proportional to $1/\rho$. ρ does not vary by much in terms of q_a except when t_d is large.

LIST OF TABLES

Table 1

Solar radiation at bottom of atmosphere in W m^{-2}

LAT	Jan	Feb	Mar	Apr	May	Jun	Jul	Aug	Sep	Oct	Nov	Dec
90°N	0.0	0.0	1.6	159.4	349.1	414.4	379.4	205.6	38.3	0.0	0.0	0.0
80°N	0.0	0.0	38.3	172.2	341.1	401.7	366.6	213.6	68.5	8.0	0.0	0.0
70°N	0.0	25.5	95.6	208.8	326.8	376.2	337.9	232.7	119.6	43.0	8.0	0.0
60°N	28.7	68.5	157.8	255.4	331.6	365.0	341.1	266.2	180.1	97.2	41.4	17.5
50°N	76.5	130.7	212.0	294.9	353.9	377.8	360.2	304.5	229.5	154.6	92.5	62.2
40°N	140.3	194.5	261.4	323.6	366.6	382.6	373.0	333.1	271.0	210.4	154.6	122.7
30°N	199.3	247.1	296.5	341.1	366.6	379.4	373.0	347.5	304.5	256.6	208.8	183.3
20°N	247.1	285.3	322.0	344.3	358.7	363.4	360.2	344.3	325.2	294.9	256.6	234.3
10°N	288.6	315.6	336.3	337.9	337.9	334.7	336.3	328.4	337.9	320.4	294.9	279.0
0°	322.0	333.1	342.7	325.2	307.6	299.7	304.5	307.6	337.9	337.9	325.2	306.0
10°S	350.7	347.5	336.3	306.0	282.1	259.8	259.8	275.8	325.2	341.1	347.5	350.7
20°S	369.8	350.7	318.8	274.2	234.3	213.6	220.0	237.5	301.3	334.7	360.2	376.2
30°S	381.0	347.5	296.5	237.5	189.7	169.0	176.9	192.9	271.0	320.4	366.6	392.1
40°S	382.6	328.4	261.4	194.5	138.7	116.4	129.1	143.5	227.9	298.1	363.4	401.7
50°S	376.2	301.3	220.0	146.6	86.1	60.6	73.3	87.7	191.3	364.6	347.5	398.5
60°S	360.2	264.6	174.4	89.3	38.3	15.9	25.5	36.7	135.5	224.8	334.7	388.9
70°S	360.2	226.3	116.4	35.1	1.6	0.0	0.0	0.0	79.7	181.7	334.7	396.9
80°S	382.6	204.0	68.5	0.0	0.0	0.0	0.0	0.0	33.5	154.6	349.1	414.4
90°S	396.7	196.1	27.1	0.0	0.0	0.0	0.0	0.0	0.0	143.5	360.2	430.4

Table 2

Albedo of sea surface

LAT	Jan	Feb	Mar	Apr	May	Jun	Jul	Aug	Sep	Oct	Nov	Dec
90°N	0.00	0.00	0.00	0.20	0.15	0.12	0.10	0.10	0.18	0.00	0.00	0.00
80°N	0.08	0.08	0.08	0.08	0.08	0.08	0.08	0.08	0.08	0.08	0.08	0.08
70°N	0.08	0.08	0.08	0.08	0.08	0.08	0.08	0.08	0.08	0.08	0.08	0.10
60°N	0.10	0.10	0.08	0.08	0.07	0.07	0.07	0.07	0.08	0.08	0.10	0.11
50°N	0.11	0.10	0.08	0.07	0.06	0.06	0.06	0.07	0.07	0.08	0.11	0.12
40°N	0.10	0.09	0.07	0.07	0.06	0.06	0.06	0.06	0.07	0.08	0.10	0.11
30°N	0.09	0.07	0.06	0.06	0.06	0.06	0.06	0.06	0.06	0.07	0.08	0.09
20°N	0.07	0.06	0.06	0.06	0.06	0.06	0.06	0.06	0.06	0.06	0.07	0.07
10°N	0.07	0.06	0.06	0.06	0.06	0.06	0.06	0.06	0.06	0.06	0.06	0.06
0°	0.06	0.06	0.06	0.06	0.06	0.06	0.06	0.06	0.06	0.06	0.06	0.06
10°S	0.06	0.06	0.06	0.06	0.06	0.06	0.06	0.06	0.06	0.06	0.06	0.06
20°S	0.06	0.06	0.06	0.06	0.07	0.07	0.07	0.06	0.06	0.06	0.06	0.06
30°S	0.06	0.06	0.07	0.08	0.09	0.09	0.09	0.08	0.07	0.07	0.06	0.06
40°S	0.06	0.07	0.08	0.09	0.10	0.10	0.10	0.09	0.08	0.07	0.06	0.06
50°S	0.06	0.07	0.08	0.09	0.11	0.11	0.11	0.09	0.08	0.07	0.06	0.06
60°S	0.07	0.08	0.09	0.10	0.11	0.11	0.11	0.10	0.09	0.08	0.07	0.07
70°S	0.55	0.55	0.55	0.80	0.80	0.80	0.80	0.80	0.80	0.55	0.55	0.55
80°S	0.80	0.80	0.80	0.80	0.80	0.80	0.80	0.80	0.80	0.80	0.80	0.80
90°S	0.80	0.80	0.80	0.80	0.80	0.80	0.80	0.80	0.80	0.80	0.80	0.80

Table 3

Incoming solar radiation cloud cover coefficient [4]

LAT	C_s	LAT	C_s	LAT	C_s	LAT	C_s
90°	0.00	65°	0.25	40°	0.38	15°	0.39
85°	0.00	60°	0.36	35°	0.38	10°	0.40
80°	0.15	55°	0.41	30°	0.36	5°	0.40
75°	0.16	50°	0.40	25°	0.35	0°	0.38
70°	0.18	45°	0.38	20°	0.37		

Table 4

Solar radiation at 51°N

Average Cloud cover /Okt	% radiation reaching sea surface	Annual av solar radn gain /W m^{-2}
1.0	94.5	
2.0	87.7	
3.0	79.7	
4.0	70.5	
4.6	64.4	128.0
5.0	60.2	
5.6 *	53.4	106.0
6.0	48.6	
6.6	41.1	81.5
7.0	32.9	
7.6	27.7	54.9
8.0	22.0	

[4] Data applies to both northern and southern hemisphere.

Table 5

Solar radiation at 51°N and 57°N in W m^{-2}

Month	No cloud cover			Cloud cover 5.6 Okt		
	51°N	57°N	diff	51°N	57°N	diff
Jan	60.0	36.9	23.1	32.1	19.4	12.7
Apr	268.4	247.5	20.9	143.3	130.4	12.9
Jul	335.0	323.1	11.9	178.8	170.2	8.6
Oct	133.5	105.2	28.3	71.3	55.4	15.9

Table 6

Exchange coefficient data

Note these values are ×1000

WIND SPEED /m s^{-1}	AIR-SEA TEMPERATURE DIFF /°C ×1000						
	>5.0	>1.0	>0.2	>-0.2	>-1.0	>-5.0	<-5.0
=0	0.00	0.00	0.00	0.00	0.00	0.00	0.00
≤3	0.07	0.30	0.72	1.32	1.65	2.05	2.52
≤6	0.22	0.67	1.12	1.34	1.45	1.68	2.01
≤9	0.69	1.17	1.36	1.44	1.46	1.58	1.79
≤12	1.06	1.36	1.48	1.53	1.58	1.65	1.79
≤15	1.39	1.58	1.61	1.64	1.68	1.74	1.84
≤20	1.59	1.68	1.75	1.80	1.82	1.86	1.94
≤25	1.74	1.79	1.83	1.86	1.88	1.86	1.93
≤30	1.81	1.84	1.85	1.86	1.87	1.88	1.90
>30	1.86	1.86	1.86	1.86	1.86	1.86	1.86

Table 7

Long wave radiation cloud cover coefficient [5]

LAT	c_c	LAT	c_c
90°	0.88	40°	0.68
80°	0.84	30°	0.63
70°	0.80	20°	0.59
60°	0.76	10°	0.52
50°	0.72	0°	0.48

Table 8

Summary of data from Noord Hinder for year 1977

		Mean values	Std dev	Mean values [6]	Std dev
Air temp	t_a /°C	11.0	4.0		
Sea surface temp	t_s /°C	11.6	3.4		
Wet-bulb temp	t_w /°C	9.5	3.9	9.5	4.0
Dew-point temp	t_d /°C	8.3	4.2	8.3	4.3
Atm pressure	P_{atm} /Pa	101392	1361		
Relative humidity	RH /%	83.8	8.5	83.5	2.7
Correlation coeff	$t_a - t_w$	0.9813	-	0.9999	-
	$t_a - t_d$	0.9312	-	0.9998	-

[5] Data applies to both northern and southern hemisphere.

[6] Wet-bulb temperature set to be 1.41°C below air temperature.

Table 9

Heat exchange at the sea surface at 51°N

Average air temperature /°C	Average Latent heat flux /W m^{-2}	Av effective IR back radiation /W m^{-2}	Average sensible heat flux /W m^{-2}	Average annual heat exchange [7] /W m^{-2}
9.0	61.2	36.7	42.3	-34.4
10.0	59.0	37.1	25.1	-15.4
11.0 *	55.4	37.5	8.8	4.0
12.0	51.6	37.9	-5.5	21.8
13.0	48.5	38.4	-18.1	37.0
Av sea surface temperature /°C				
9.6	15.3	37.3	-18.2	71.4
10.6	33.5	37.4	-5.5	40.4
11.6 *	55.4	37.5	8.8	4.0
12.6	80.8	37.6	25.0	-37.6
13.6	107.7	37.8	42.0	-81.7
Average dew-point temperature /°C				
6.6 RH 75%	82.7	38.7	8.85	-24.5
8.0 RH 82%	60.5	37.7	8.85	-1.3
8.3 RH 83% *	55.4	37.5	8.85	4.0
9.4 RH 90%	36.2	36.7	8.84	24.0
10.8 RH 99%	9.8	35.7	8.84	51.4
Average wind speed /m s^{-1}				
4.8	35.1	37.5	5.6	27.6
6.3	44.8	37.5	7.1	16.4
7.8 *	55.4	37.5	8.8	4.0
9.3	70.2	37.5	11.2	-13.1
10.8	81.6	37.5	13.0	-26.3
Average pressure /Pa				
100 000	55.46	37.53	8.73	4.1
101 392 *	55.44	37.53	8.85	4.0
102 000	55.44	37.53	8.90	3.9
Average cloud cover /Okt				
4.6	55.4	44.3	8.8	19.2
5.6 *	55.4	37.5	8.8	4.0
6.6	55.4	30.7	8.8	-13.4
7.6	55.4	23.9	8.8	-33.2

[7] Negative values mean that the sea undergoes a net heat loss.

Table 10

Heat exchange with respect to air and sea surface temperature

Av sea srfce temp /°C	Average air temperature /°C									
	9.0		10.0		11.0 *		12.0		13.0	
9.6	L_e	17.5	L_e	16.3	L_e	15.3	L_e	14.7	L_e	14.1
	IR	36.5	IR	36.9	IR	37.3	IR	37.7	IR	38.1
	S	8.9	S	-5.5	S	-18.2	S	-30.0	S	-40.8
	H_x	**42.9**	**H_x**	**58.1**	**H_x**	**71.4**	**H_x**	**83.4**	**H_x**	**94.4**
10.6	L_e	38.3	L_e	36.0	L_e	33.5	L_e	31.5	L_e	30.2
	IR	36.6	IR	37.0	IR	37.4	IR	37.8	IR	38.2
	S	25.2	S	8.9	S	-5.5	S	-18.1	S	-29.9
	H_x	**5.7**	**H_x**	**23.9**	**H_x**	**40.4**	**H_x**	**54.6**	**H_x**	**67.3**
11.6 *	L_e	61.2	L_e	59.0	L_e	55.4	L_e	51.6	L_e	48.5
	IR	36.7	IR	37.1	IR	37.5	IR	37.9	IR	38.4
	S	42.3	S	25.1	S	8.8	S	-5.5	S	-18.1
	H_x	**-34.4**	**H_x**	**-15.4**	**H_x**	**4.0**	**H_x**	**21.8**	**H_x**	**37.0**
12.6	L_e	86.9	L_e	83.9	L_e	80.8	L_e	75.9	L_e	70.6
	IR	36.8	IR	37.2	IR	37.6	IR	38.1	IR	38.5
	S	60.4	S	42.1	S	25.0	S	8.8	S	-5.5
	H_x	**-78.3**	**H_x**	**-57.4**	**H_x**	**-37.6**	**H_x**	**-17.0**	**H_x**	**2.2**
13.6	L_e	115.5	L_e	111.6	L_e	107.7	L_e	103.8	L_e	97.5
	IR	36.9	IR	37.3	IR	37.8	IR	38.2	IR	38.6
	S	79.5	S	60.2	S	42.0	S	24.9	S	8.8
	H_x	**-126.1**	**H_x**	**-103.3**	**H_x**	**-81.7**	**H_x**	**-61.1**	**H_x**	**-39.1**

KEY: L_e Latent heat flux

IR Effective infra-red back radiation

S Sensible heat flux

H_x Average annual heat flux

* annual average values (Noord Hinder 1977)

Average wind speed and cloud cover values from Isemer & Hasse, 7.8 m s^{-1} and 5.6 Okt respectively.

Values are calculated by treating each variable as being independent - all other variables are held constant.

LIST OF FIGURES

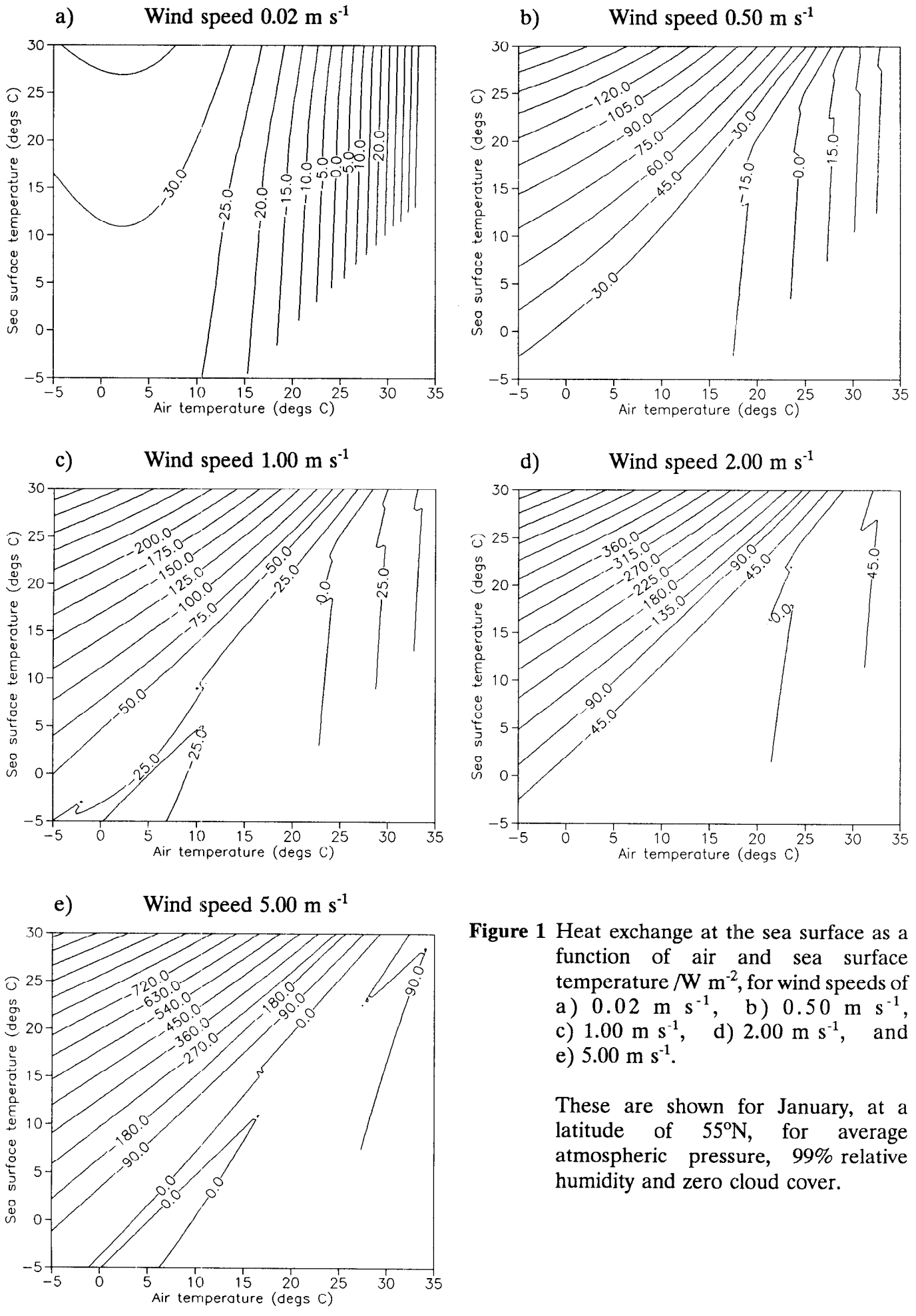

Figure 1 Heat exchange at the sea surface as a function of air and sea surface temperature /W m^{-2}, for wind speeds of a) 0.02 m s^{-1}, b) 0.50 m s^{-1}, c) 1.00 m s^{-1}, d) 2.00 m s^{-1}, and e) 5.00 m s^{-1}.

These are shown for January, at a latitude of 55°N, for average atmospheric pressure, 99% relative humidity and zero cloud cover.

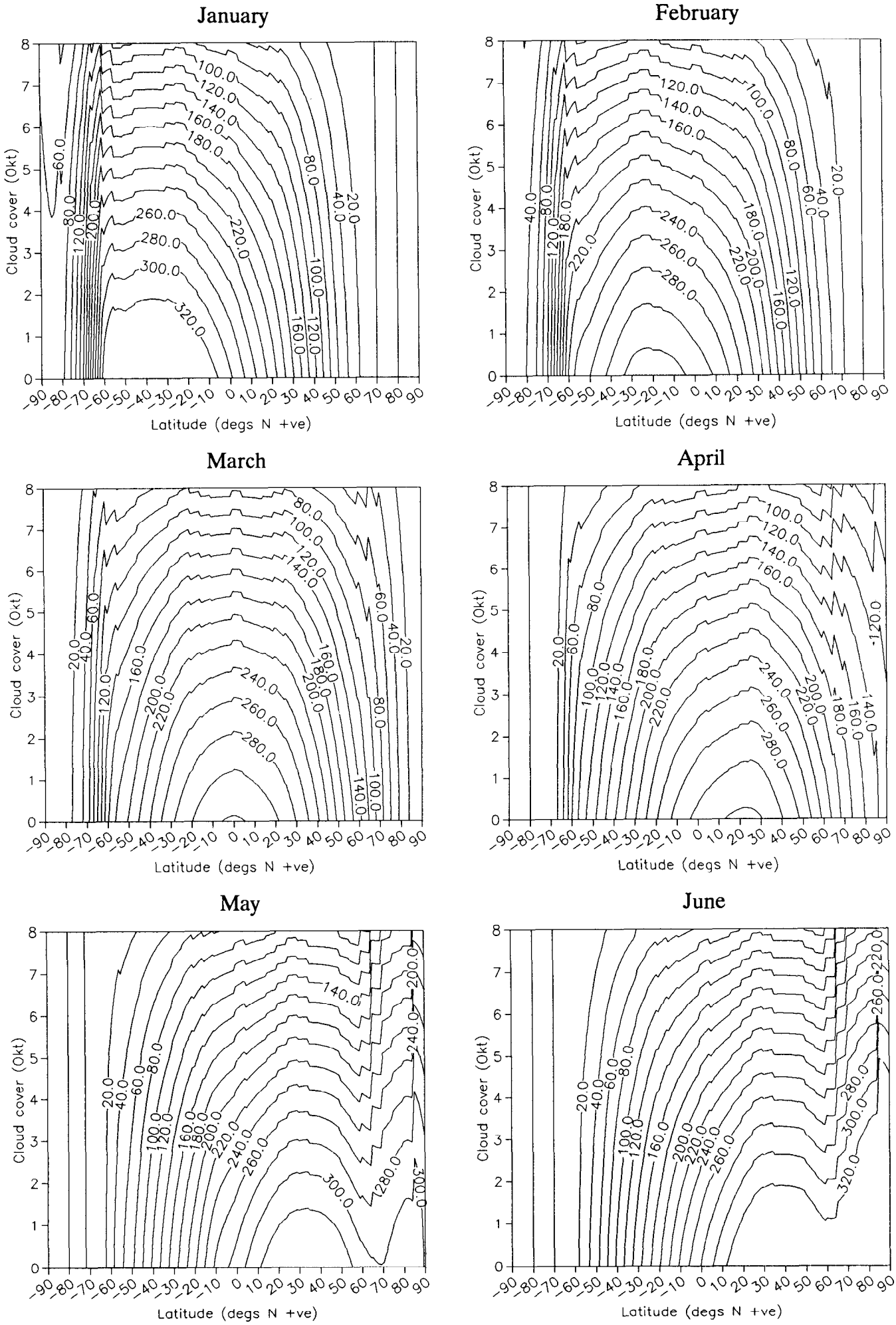

Figure 2 (Jan - Jun) Solar radiation flux at the sea surface as a function of cloud cover and latitude /W m^{-2}

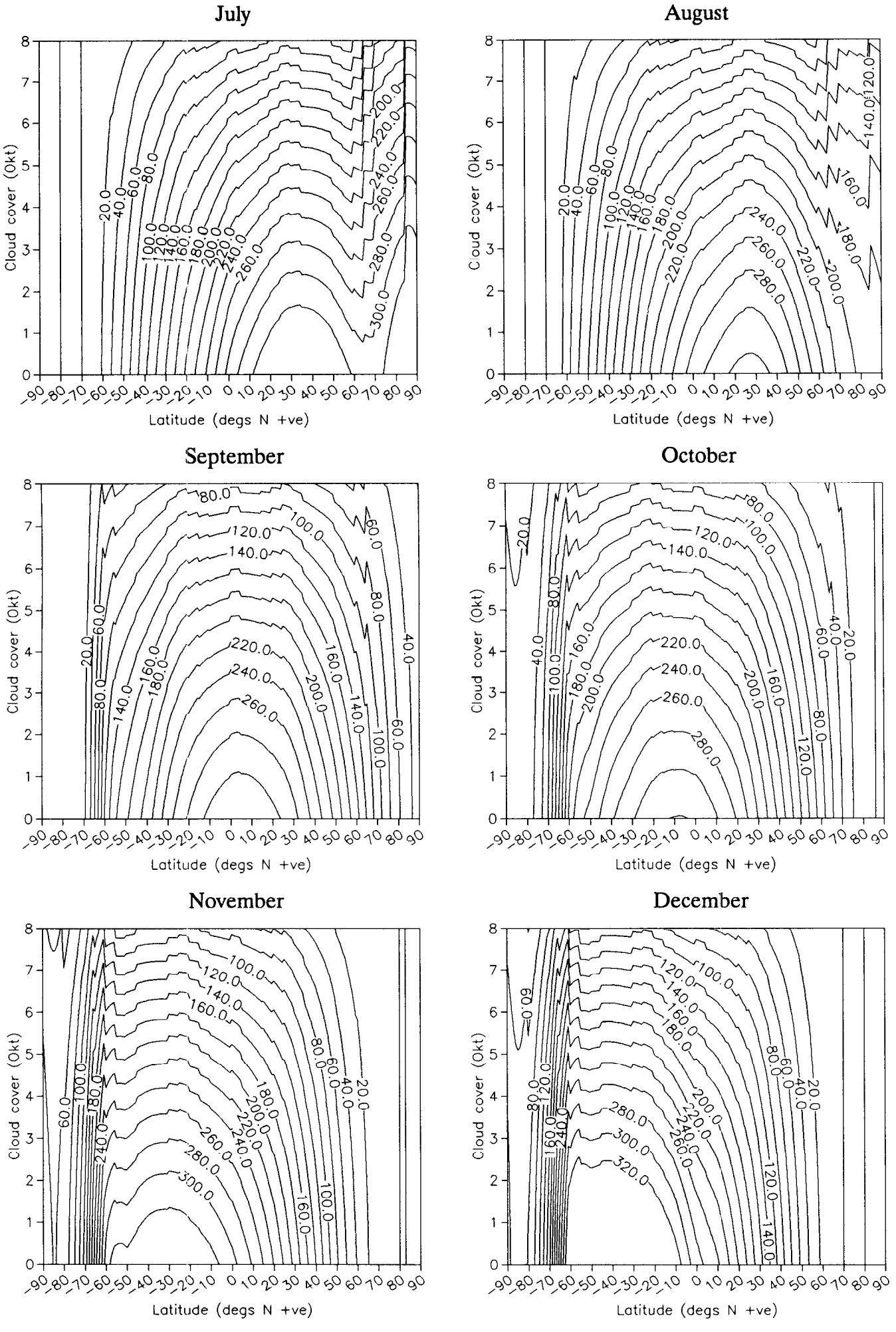

Figure 2 (Jul - Dec) Solar radiation flux at the sea surface as a function of cloud cover and latitude /W m^{-2}

a) Dew-point temperature 8.3°C
Exch coeff not interpolated

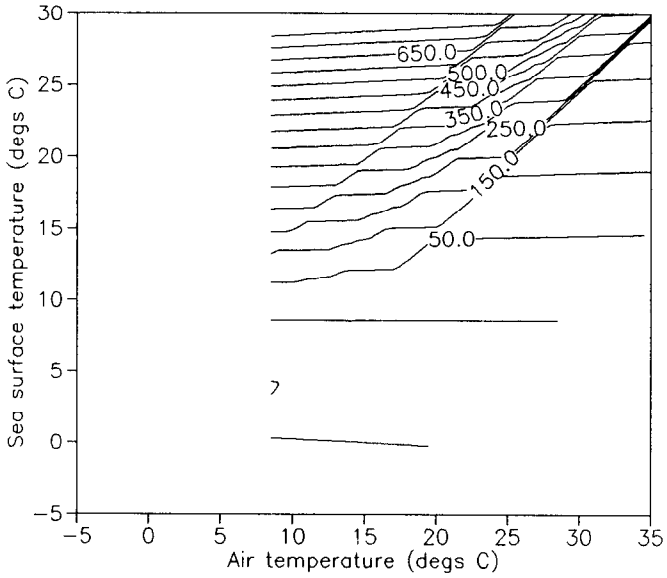

b) Dew-point temperature 8.3°C
Exch coeff linearly interpolated

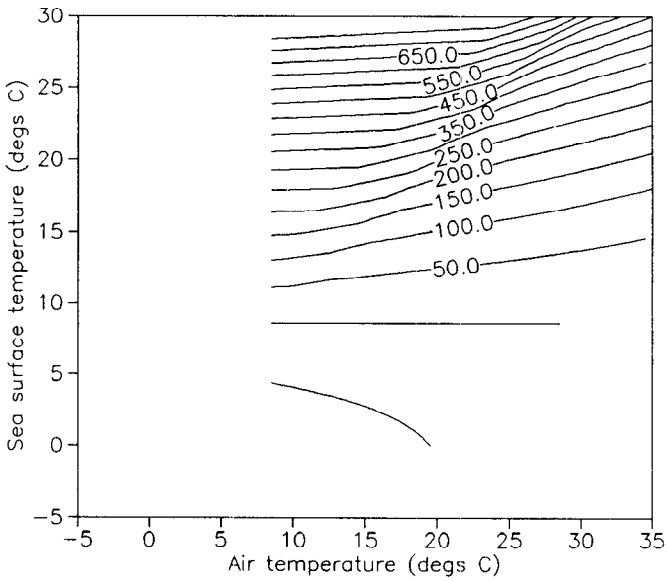

c) Dew-point temperature 6.6°C
Exch coeff linearly interpolated

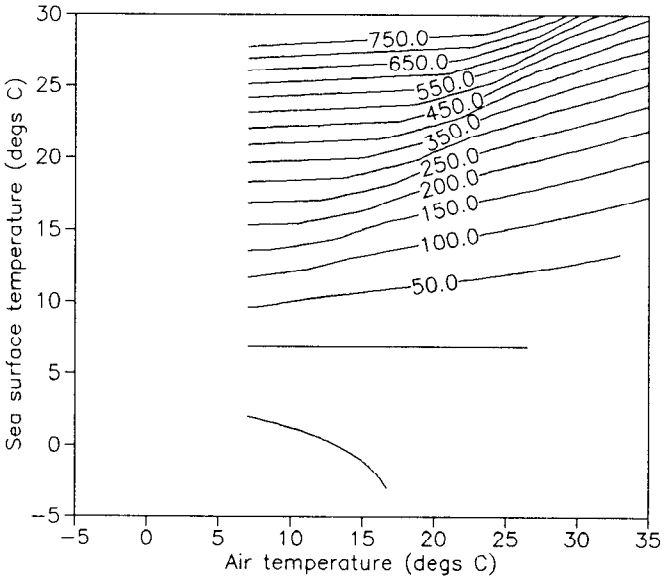

Figure 3 (a - c) Latent heat flux at the sea surface as a function of air and sea surface temperature /W m^{-2}, at a *dew-point temperature* of a) 8.3°C without interpolating the exchange coefficient, b) 8.3°C with the exchange coefficient linearly interpolated, c) 6.6°C exchange coefficient linearly interpolated.

The above are for atmospheric pressure of 101392 Pa, and wind speed of 7.8 m s^{-1}.

d) Dew-point depression 4.4°C

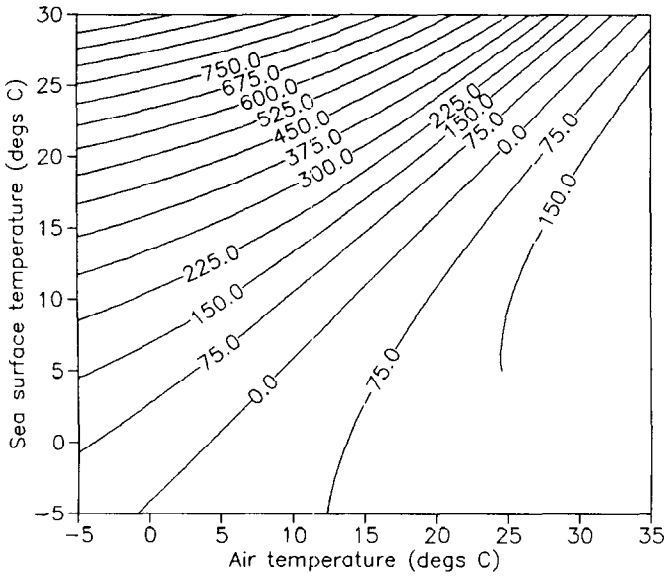

e) Dew-point depression 2.7°C

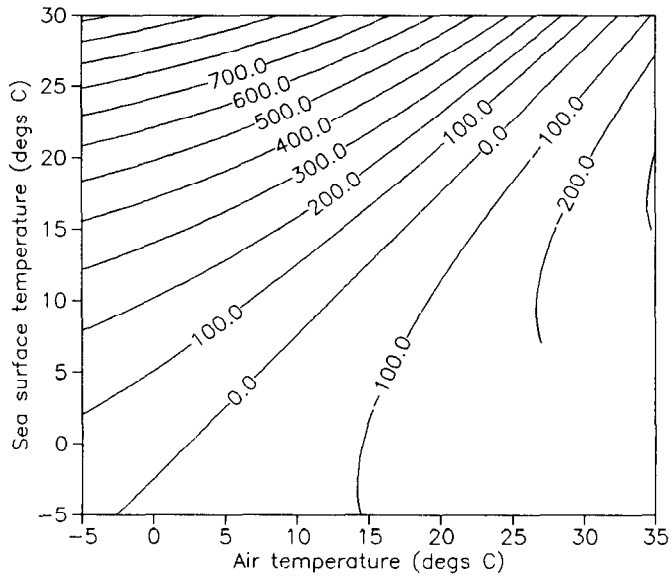

f) Dew-point depression 0.1°C

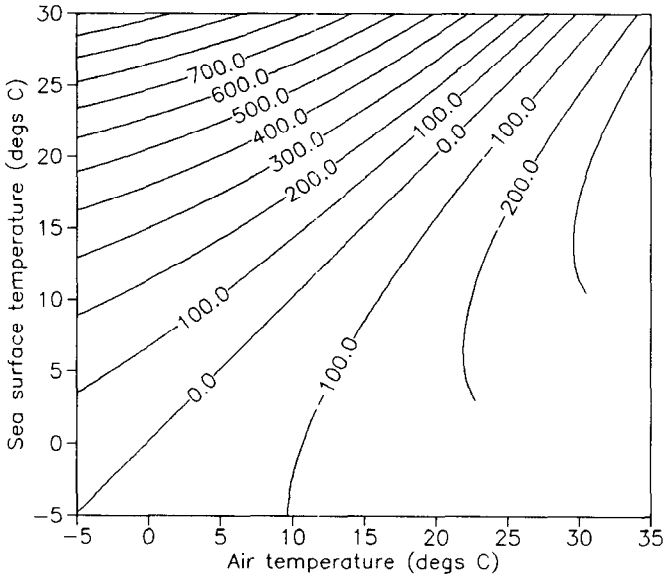

Figure 3 (d - f) Latent heat flux at the sea surface as a function of air and sea surface temperature /W m^{-2}, at a *dew-point depression* of a) 4.4°C corresponding to a relative humidity of ≈75%, b) 2.7°C R. humidity ≈83%, and c) 0.1°C R. humidity ≈99%.

The above are for atmospheric pressure of 101392 Pa, and wind speed of 7.8 m s^{-1}. In this, and subsequent figures, the exchange coefficient is linearly interpolated.

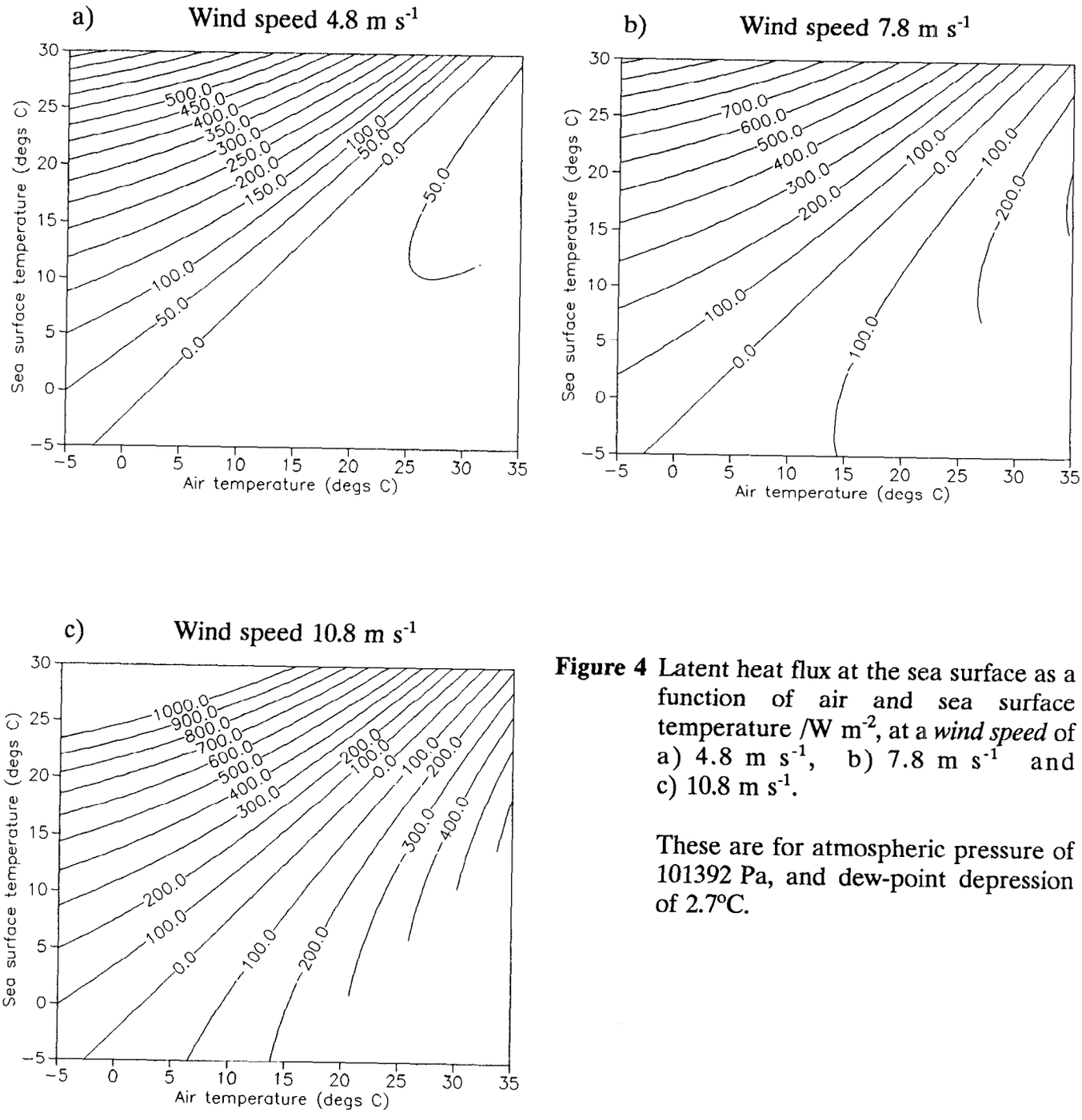

Figure 4 Latent heat flux at the sea surface as a function of air and sea surface temperature /W m^{-2}, at a *wind speed* of a) 4.8 m s^{-1}, b) 7.8 m s^{-1} and c) 10.8 m s^{-1}.

These are for atmospheric pressure of 101392 Pa, and dew-point depression of 2.7°C.

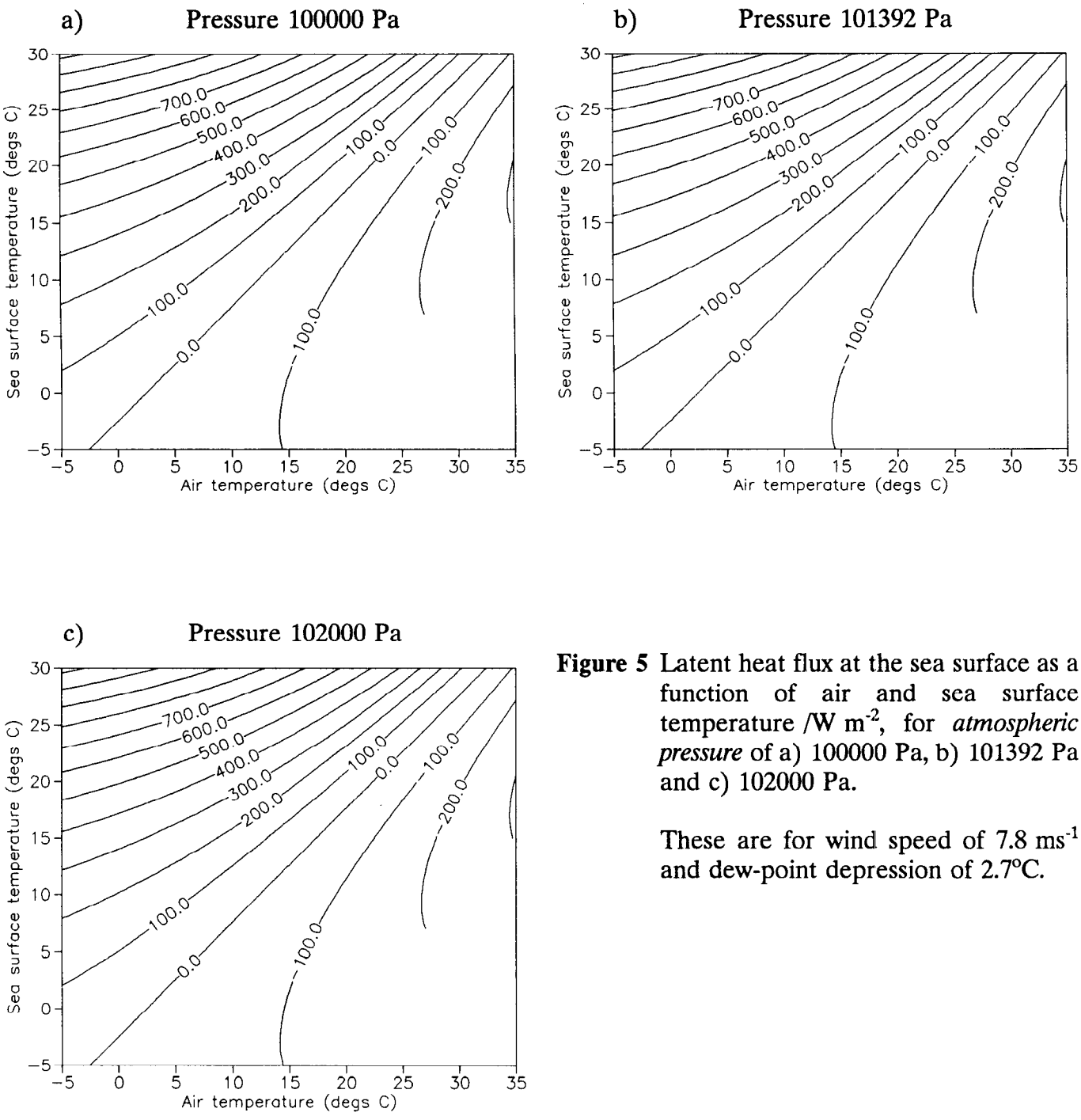

Figure 5 Latent heat flux at the sea surface as a function of air and sea surface temperature /W m^{-2}, for *atmospheric pressure* of a) 100000 Pa, b) 101392 Pa and c) 102000 Pa.

These are for wind speed of 7.8 ms^{-1} and dew-point depression of 2.7°C.

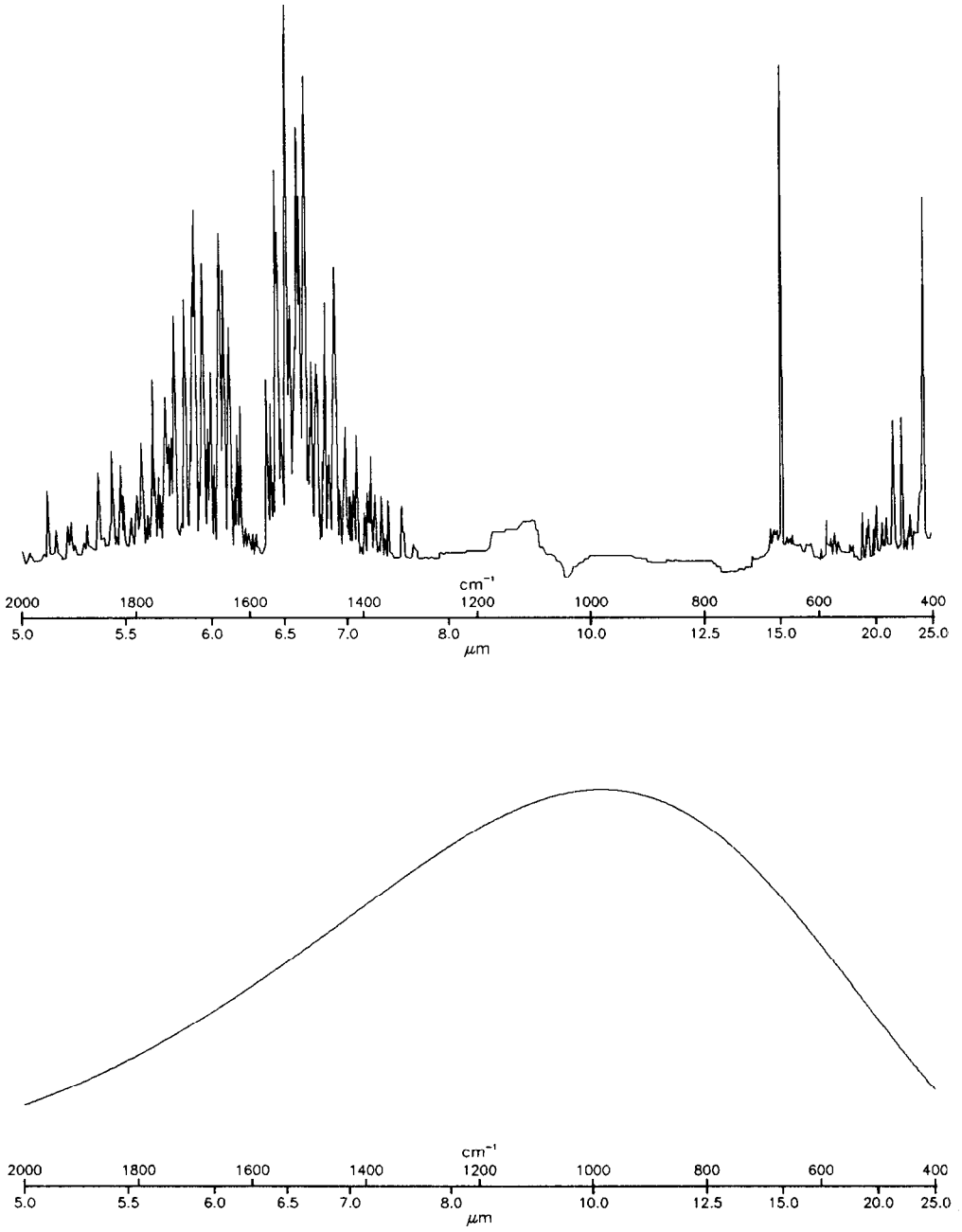

Figure 6 The infra-red spectrum of atmospheric water and carbon dioxide (above). Below is the black-body radiation spectrum at 283 K (not to same vertical scale). These show that about 50% of the black-body radiation coincides with the water and CO_2 IR spectra.

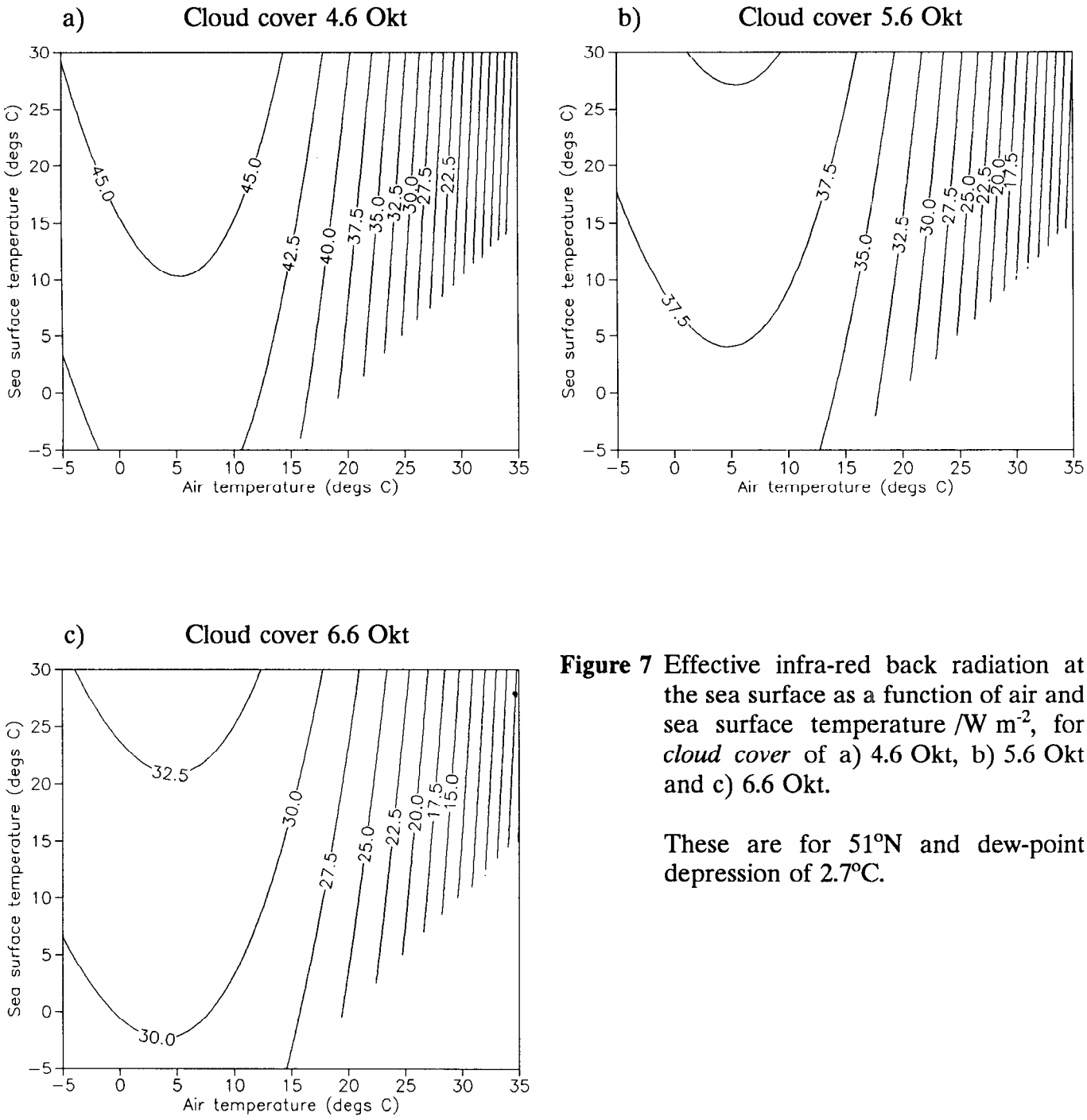

Figure 7 Effective infra-red back radiation at the sea surface as a function of air and sea surface temperature /W m^{-2}, for *cloud cover* of a) 4.6 Okt, b) 5.6 Okt and c) 6.6 Okt.

These are for 51°N and dew-point depression of 2.7°C.

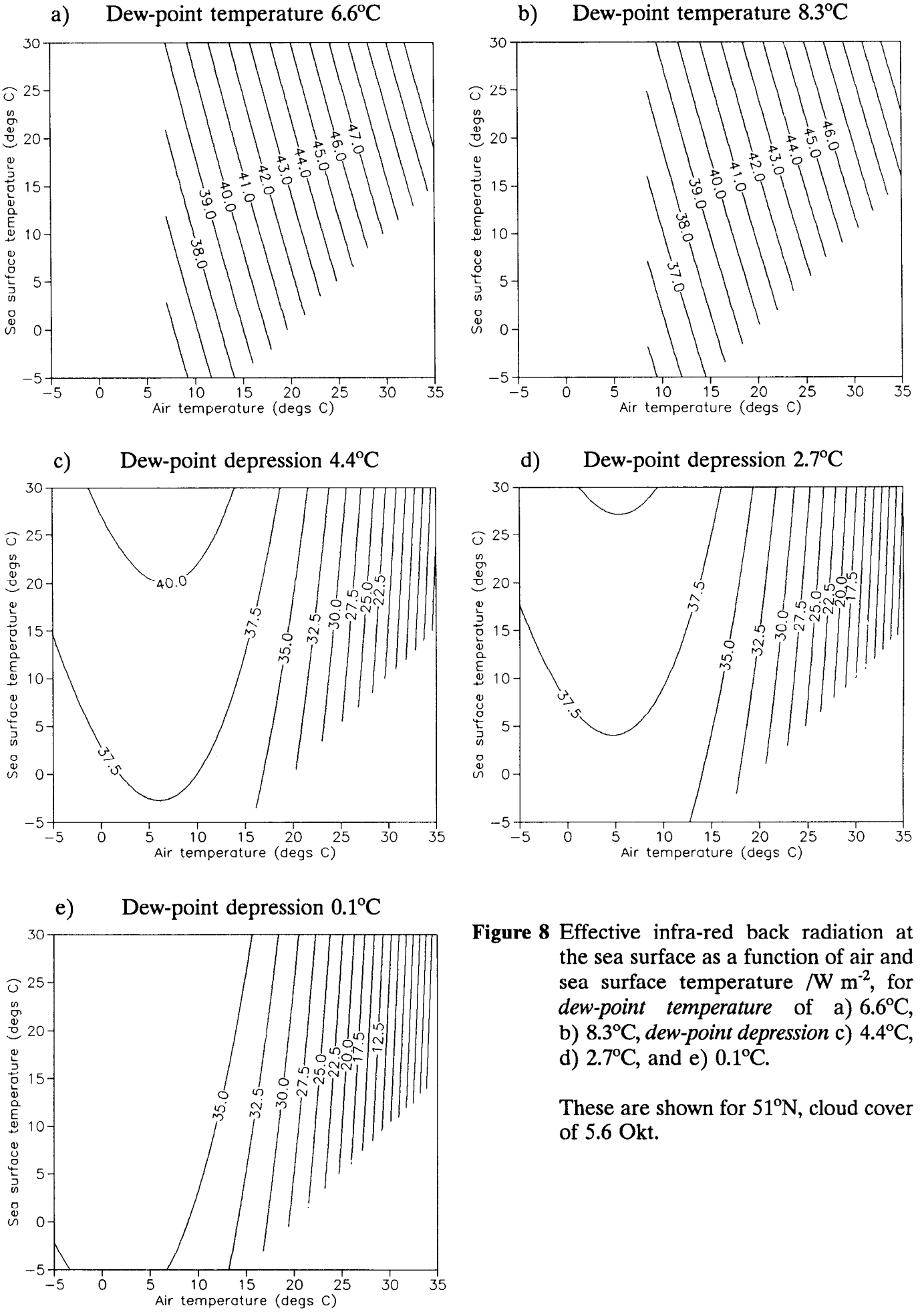

Figure 8 Effective infra-red back radiation at the sea surface as a function of air and sea surface temperature /W m^{-2}, for *dew-point temperature* of a) 6.6°C, b) 8.3°C, *dew-point depression* c) 4.4°C, d) 2.7°C, and e) 0.1°C.

These are shown for 51°N, cloud cover of 5.6 Okt.

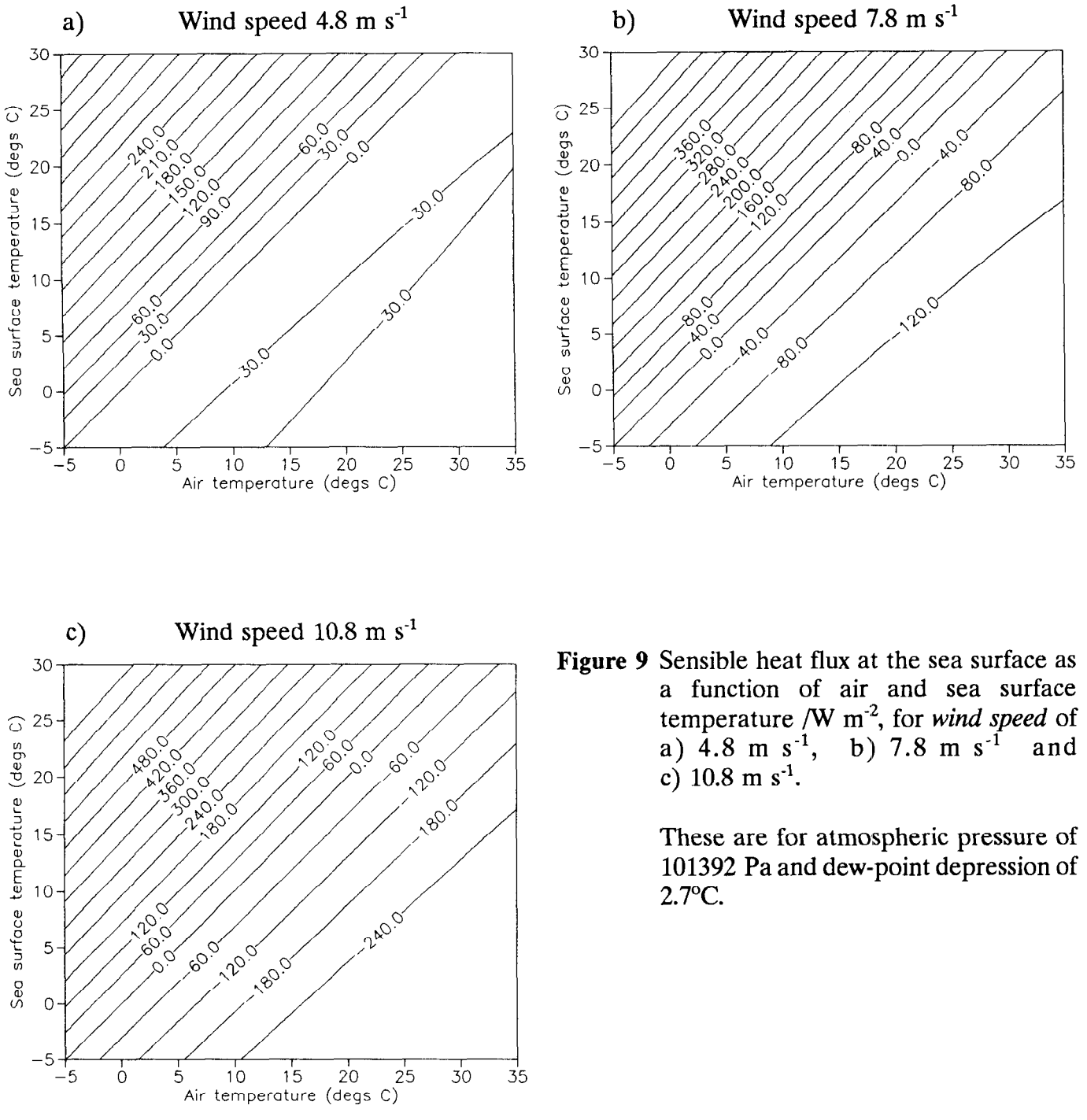

Figure 9 Sensible heat flux at the sea surface as a function of air and sea surface temperature /W m^{-2}, for *wind speed* of a) 4.8 m s^{-1}, b) 7.8 m s^{-1} and c) 10.8 m s^{-1}.

These are for atmospheric pressure of 101392 Pa and dew-point depression of 2.7°C.

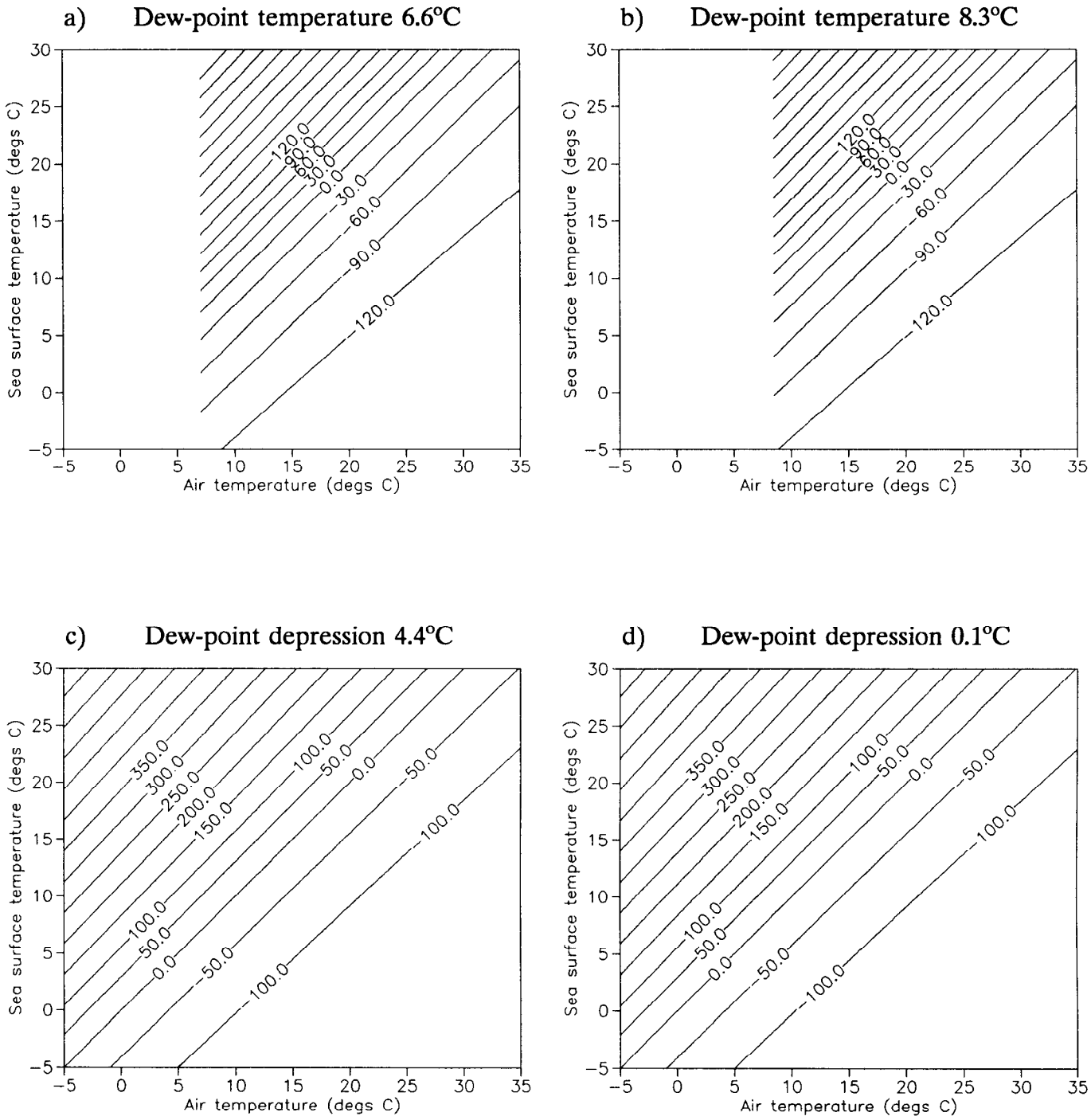

Figure 10 Sensible heat flux at the sea surface as a function of air and sea surface temperature /W m^{-2}, for *dew-point temperature* of a) 8.3°C, b) 6.6°C and *dew-point depression* c) 4.4°C and d) 0.1°C.

The above are for atmospheric pressure of 101392 Pa and wind speed of 7.8 m s^{-1}. These plots sho that the sensible heat flux is insensitive to changes in dew-point temperature, except when the dew-point temperature is high.

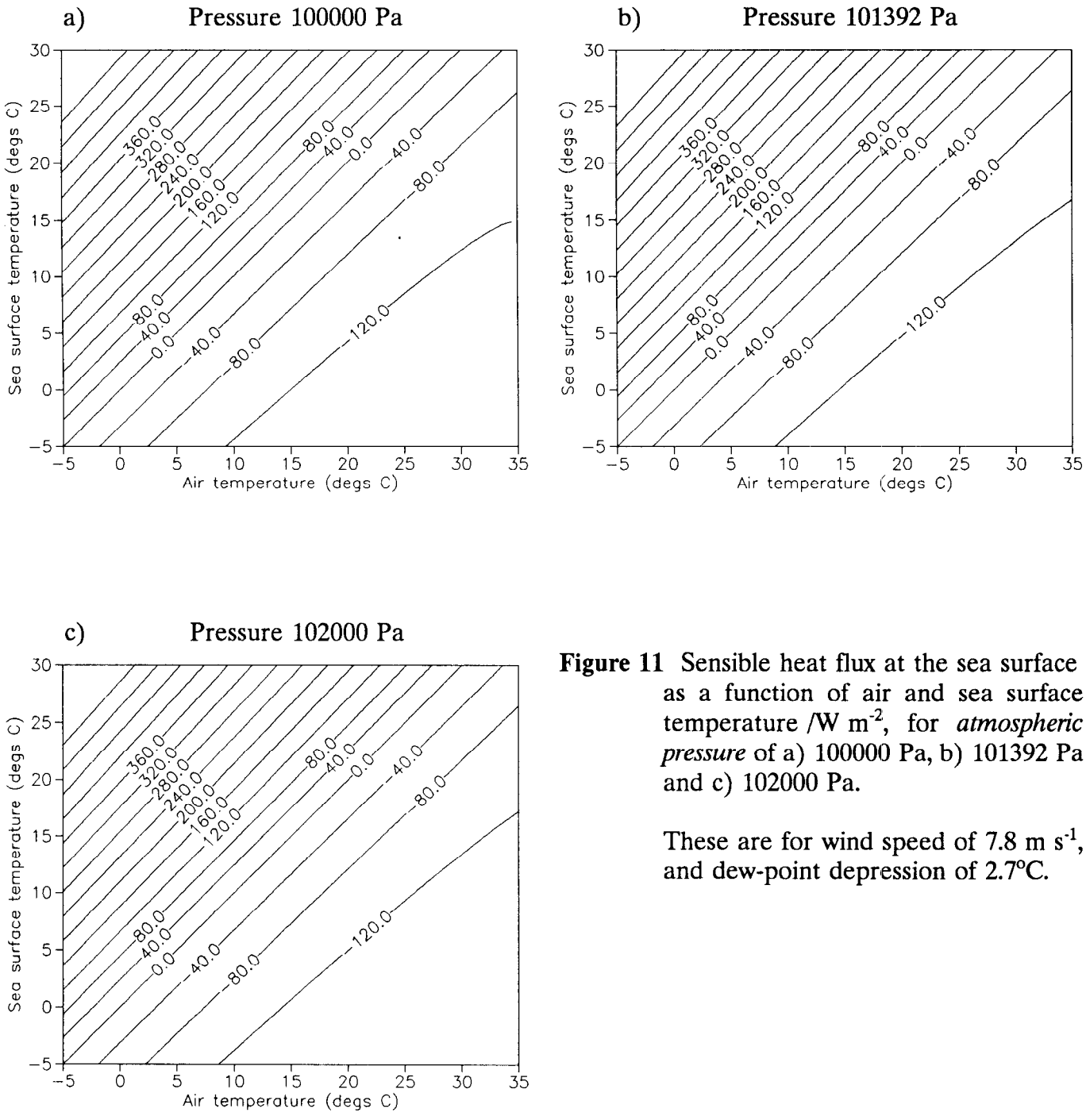

Figure 11 Sensible heat flux at the sea surface as a function of air and sea surface temperature /W m^{-2}, for *atmospheric pressure* of a) 100000 Pa, b) 101392 Pa and c) 102000 Pa.

These are for wind speed of 7.8 m s^{-1}, and dew-point depression of 2.7°C.

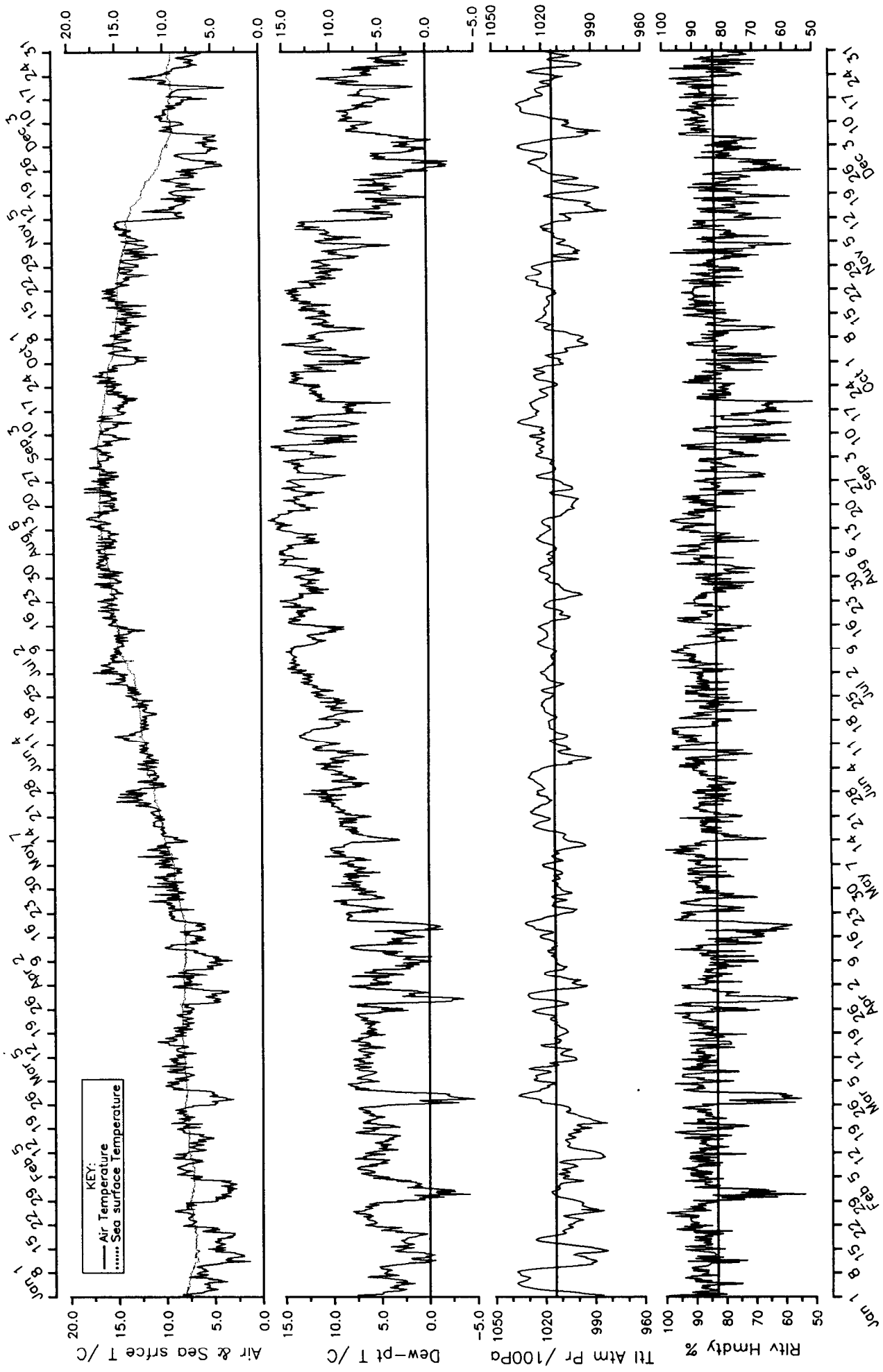

Figure 12 Annual cycle: data from Noord Hinder for 1977.

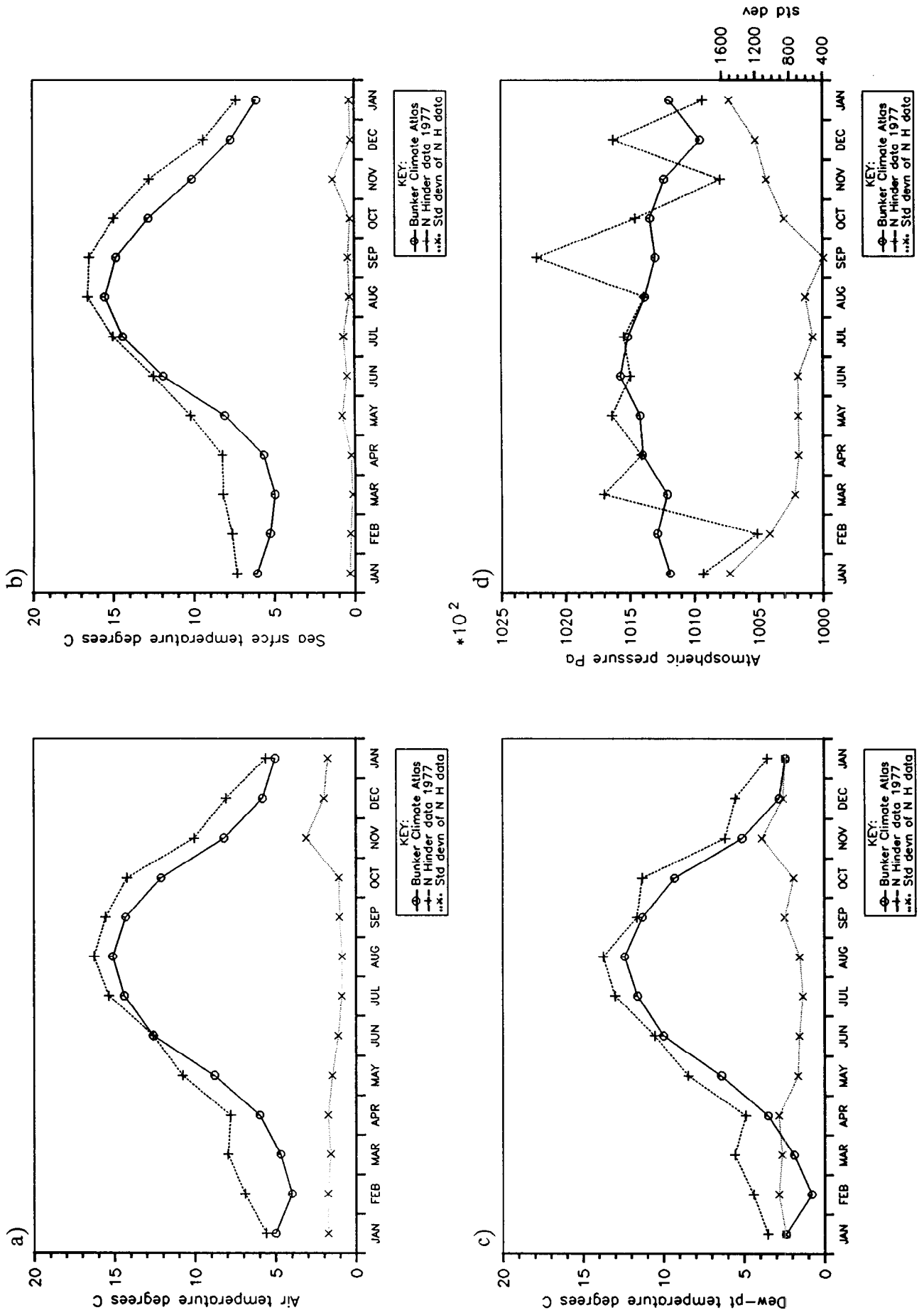

Figure 13 Comparison of the annual cycle of data from Noord Hinder, with data from the Bunker Climate Atlas for a) air temperature, b) sea surface temperature, c) dew-point temperature and d) atmospheric pressure.

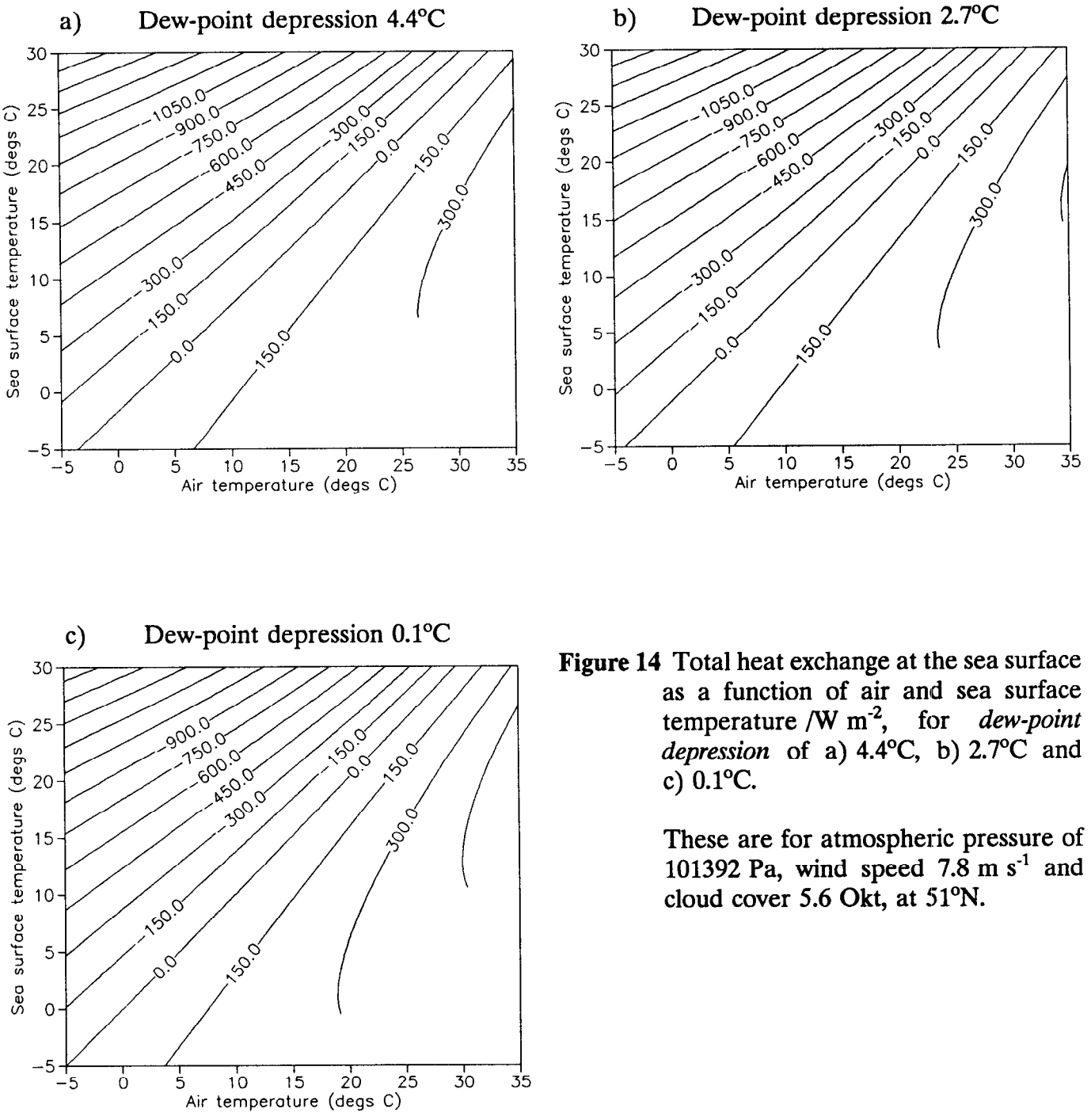

Figure 14 Total heat exchange at the sea surface as a function of air and sea surface temperature /W m^{-2}, for *dew-point depression* of a) 4.4°C, b) 2.7°C and c) 0.1°C.

These are for atmospheric pressure of 101392 Pa, wind speed 7.8 m s^{-1} and cloud cover 5.6 Okt, at 51°N.

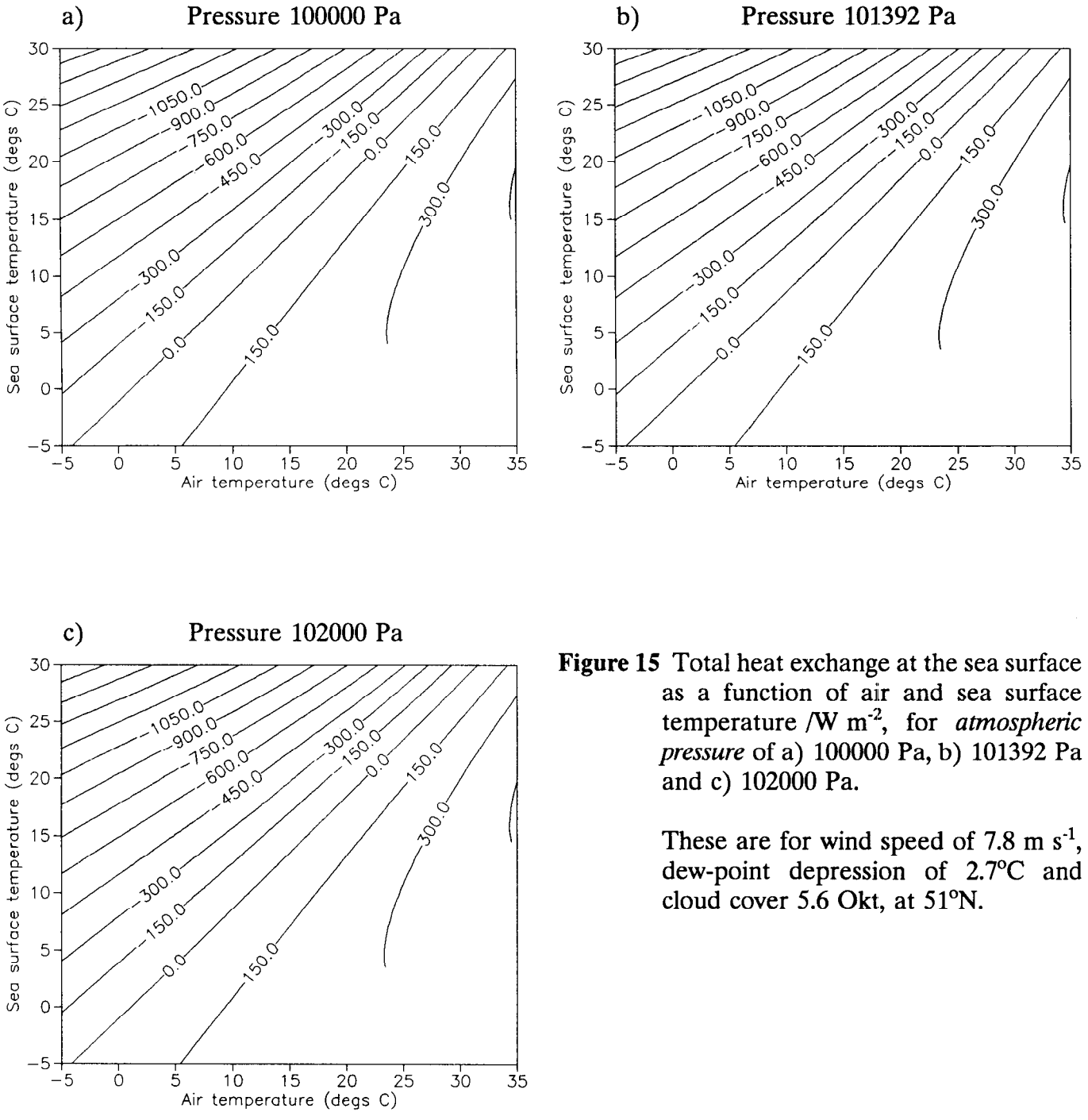

Figure 15 Total heat exchange at the sea surface as a function of air and sea surface temperature /W m^{-2}, for *atmospheric pressure* of a) 100000 Pa, b) 101392 Pa and c) 102000 Pa.

These are for wind speed of 7.8 m s^{-1}, dew-point depression of 2.7°C and cloud cover 5.6 Okt, at 51°N.

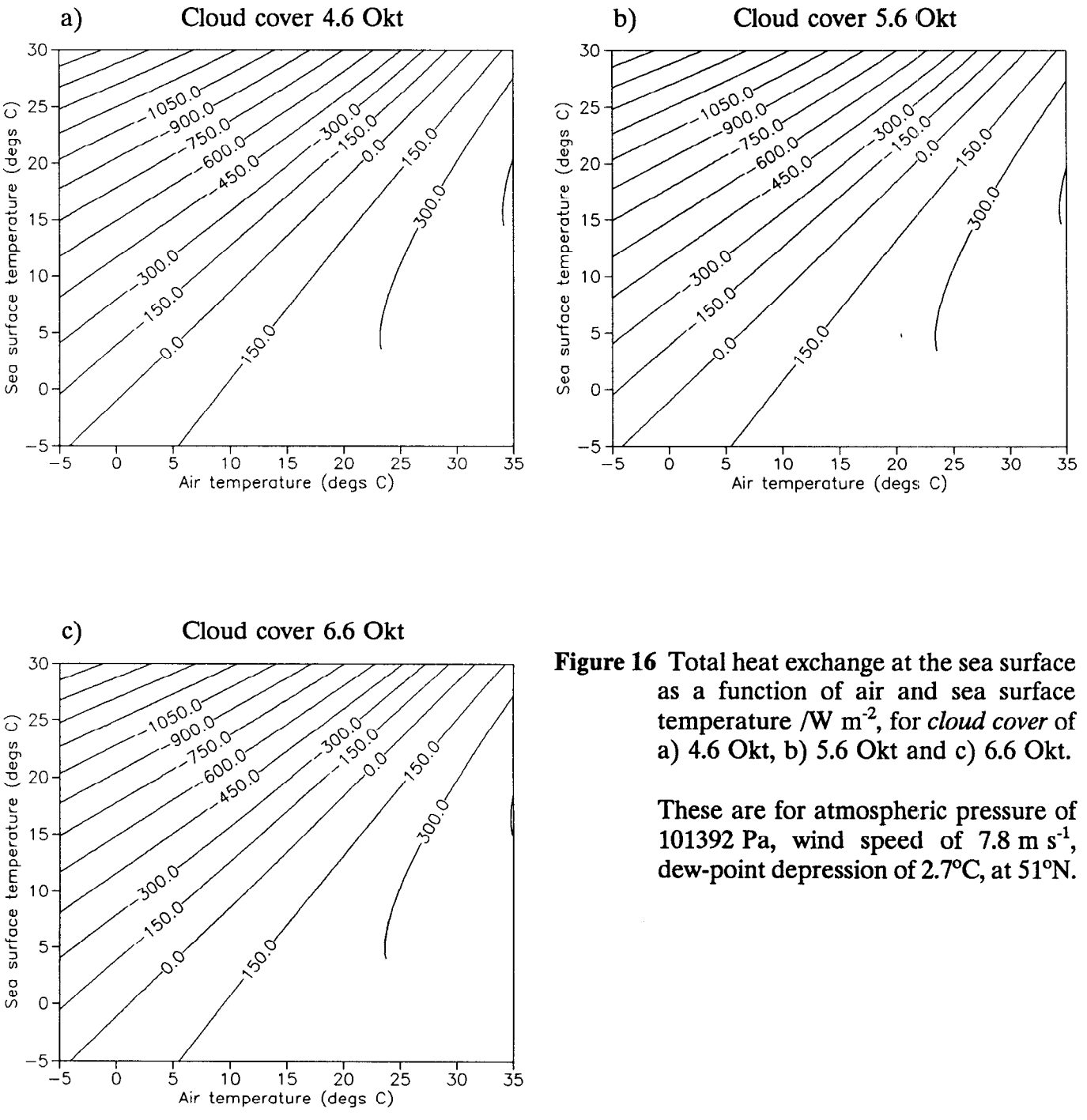

Figure 16 Total heat exchange at the sea surface as a function of air and sea surface temperature /W m^{-2}, for *cloud cover* of a) 4.6 Okt, b) 5.6 Okt and c) 6.6 Okt.

These are for atmospheric pressure of 101392 Pa, wind speed of 7.8 m s^{-1}, dew-point depression of 2.7°C, at 51°N.

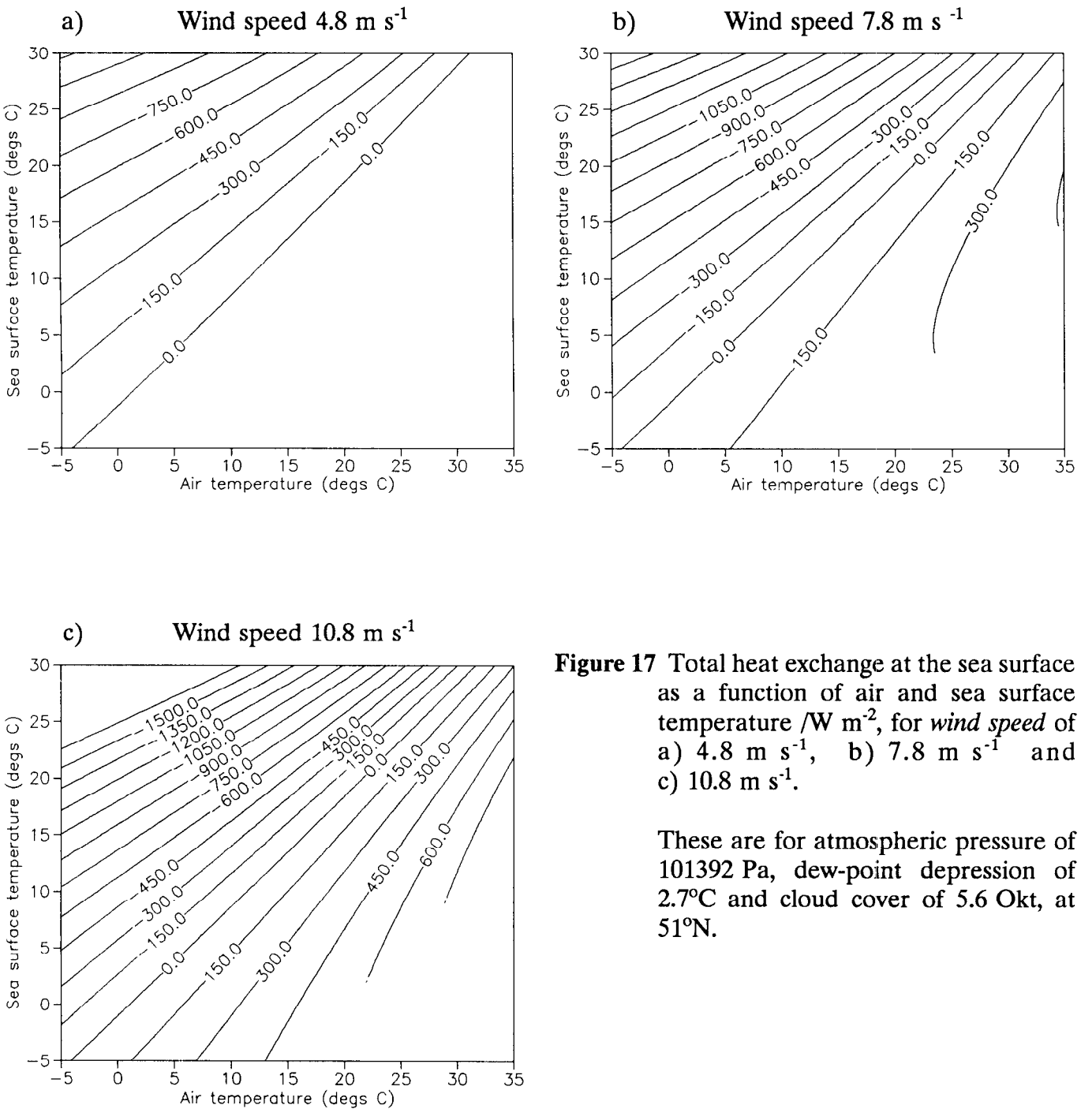

Figure 17 Total heat exchange at the sea surface as a function of air and sea surface temperature /W m^{-2}, for *wind speed* of a) 4.8 m s^{-1}, b) 7.8 m s^{-1} and c) 10.8 m s^{-1}.

These are for atmospheric pressure of 101392 Pa, dew-point depression of 2.7°C and cloud cover of 5.6 Okt, at 51°N.